運輸省港湾技術研究所

港湾技術研究所報告

REPORT OF THE PORT AND HARBOUR RESEARCH INSTITUTE

MINISTRY OF TRANSPORT

VOL. 15 NO. 2 JUNE 1976

NAGASE, YOKOSUKA, JAPAN

港湾技術研究所報告 (REPORT OF P.H.R.I.)

第15巻 第2号 (Vol. 15, No. 2), 1976年6月 (June 1976)

目　次 (CONTENTS)

REPORT OF THE PORT &
HARBOUR RESEARCH INSTITUTE
Vol. 15, No. 2 (June 1976)

1. Theory of Transient Fluid Waves in a Vibrated Storage Tank

Tomotsuka TAKAYAMA*

Synopsis

Presently, many undersea storage tanks are under construction or being planned, but seismic forces are not being considered as a design force, because its computation method has not been established yet.

As an approach to the analysis of the seismic forces this paper deals with the problem of transient fluid waves which are going to develop inside a tank. In the paper, theoretical formulas for internal waves and dynamic fluid pressures in the transient state have been derived under the assumption that the tank is completely filled with two different fluids and forced to move vertically and horizontally at the same time. For the case without vertical movement, the complete analytical solution can be readily obtained; but in the case of concurrence of horizontal and vertical movements, resonant conditions are investigated by an approximate solution. Consequently, it is made clear that the vertical movement plays as important a role in the resonance phenomenon as the horizontal movement. If the natural frequencies of the fluid inside the tank are low and the tank is forced to move with high frequency, the resonance phenomena may even appear under the condition of $\omega_n=|\gamma-\Omega|$, where ω_n is the n-th natural angular frequency, and γ and Ω are the angular frequencies of the vertical and the horizontal tank oscillations, respectively.

The theory is applicable to the same problem of a ground storage tank. The validity of the theory is confirmed by experiments on rectangular and circular ground tanks which were vibrated in the horizontal direction only. The experiments also confirm that the solution for a rectangular tank is applicable to the computation of the propagation of waves generated by a piston type wave paddle.

* Chief of the Storm Surge and Tsunami Laboratory, Hydraulic Engineering Division

港湾技術研究所報告
第15巻 第2号 (1976. 6)

1. 振動外力を受けるタンク内発生波の非定常解について

高山知司*

要　旨

振動外力によってタンクが同時に鉛直および水平方向に振動された場合にタンク内部に発生する波およびタンク側壁に働く流体圧の理論式を導いた。この理論はタンク内の流体運動の過渡領域における解を与え，地震によって振動する海中タンクや地上タンクの問題に適用できる。

鉛直振動がない場合については，完全な解析解を得た。鉛直と水平振動が同時に起る場合については，近似解を求め，タンク内の流体の共振条件について検討した。その結果，水平振動と同様に鉛直振動もタンク内の液体の共振に対して重要な要素となることがわかった。

この理論の妥当性は，矩形や円形の地上タンクの模型実験によって確認された。さらに，矩形タンクに対する理論は，ピストンタイプの造波板によって発生された波の伝播状況の計算にも適用できることが実験によって確認された。

* 水工部　高潮津波研究室長

Contents

1. Introduction

In Japan, an oil storage law was established in 1975 in order to provide sufficient oil supply to fundamental industry and to prevent the people from being disturbed by a goods scarcity due to a temporary oil crisis. The law obliges oil companies to reserve a sufficient quantity of petroleum which assures 90 days' oil supply. In order to accomplish the obligation by 1981, a very large area of nearly 50 square kilometers is needed for the construction of new oil storage tanks[1]. Given our small country, it is impossible to provide the wide space even if the storage is necessary at nearly any cost for our national economy. Therefore, the utilization of the sea may become necessary for the purpose of long time petroleum storage.

The development of oil resources in the sea has compelled many other coutries to construct temporary offshore oil storage tanks used as oil transport station. In consequence, many offshore structures are being planned or already under construction in area like the North Sea, the Arabian Gulf, off the Java and so on [1,2,3,4].

The discovery of large oil fields in the North Sea has particularly promoted the construction technique of sea tanks. However, the application of the present engineering technique to Japan is dangerous, because of the different environmental conditions encountered there.

The problem of earthquakes is especially important among those differences. Other countries which have a plan of sea tanks have rarely been attacked by large earthquakes, while Japan has frequently suffered from them. Consequently in those other countries, seismic forces are almost never considered in the practical design of sea tanks, and the external design forces are generally determined by wave forces in the heaviest storm, (though the importance of earthquakes is described in some engineering rules or recommendations concerning the sea tank). Another reason for neglect of seismic forces in design is that the computation method of those forces has not been established at present. Therefore, the development of the computation method is a pressing need for the construction of oil storage tanks in seismic area.

Since an undersea storage tank is surrounded by sea water and completely filled with water and oil, two types of dynamic fluid pressures are developed by the tank oscillations and act upon the structure; one is a fluid pressure by surrounding water and the other is wave pressure produced inside the tank by the waves excited on the boundary surface between the oil and the water. The former may be estimated by the solution of the steady state conditions, but in the latter, the analysis of the transient state is required, because the duration of an earthquake is not long enough for the phenomena inside the tank to reach a steady state.

As an approach to the analysis of the latter problem this paper deals with the theoretical analysis of transient fluid waves in a tank. The theory derived in the paper is applicable to the transient phenomena inside a ground and an undersea storage tank. The application of the theory is restricted only to a rectangular or a circular tank. The theory is verified by some experiments for the model ground tanks.

2. Literature Survey

Since the dynamic fluid pressures excited by earthquakes are important in the design of structures such as dams, ground tanks, and sea tanks, many analytical methods have been developed to analyze them. Most, however, deal with dams or ground tanks, and estimate the magnitude of the dynamic fluid pressures in a steady state condition. The papers which deal with the transient phenomena inside a tank are rare.

First, Westergaard[5], taking water as a compressible fluid, obtained a formula which gives the fluid pressure on a rectangular dam in a steady state condition. Then, Jacobson[6] solved the corresponding problem for a circular tank which partially contained water. He assumed that the tank was shaken in a horizontal direction only, ignored the convective terms of the acceleration in Euler's equation and therefore kept the fluid surface still. His solution of the dynamic fluid pressure p_i at a point (r, θ) is expressed as

$$p_i=-\rho f''_H(t)\cos\theta\sum_{n=1}^{\infty}A_{2n-1}J_1[i(2n-1)kr]\cos(2n-1)kz, \qquad (1)$$

where ρ denotes the density of the fluid, $f''_H(t)$ is the horizontal acceleration, θ is the angle measured from the acting direction of the earthquake, z is the vertical coordinate positive upwards, $J_1(ink_nr)$ is a Bessel function of the first kind and $k=\pi/2h$, where h is the water depth. The coefficient A_n is determined from the boundary conditions (rigid tank wall, $r=r_0$) thus:

$$A_{2n-1}=(-1)^{n+1}\frac{4}{\pi k}\frac{1/(2n-1)^2}{J_0[i(2n-1)kr_0]-\frac{1}{(2n-1)kr_0}J_1[i(2n-1)kr_0]}. \qquad (2)$$

Taking his assumptions into account, Eq. (1) is applicable only for short initial time. He also solved the dynamic fluid pressure for the case of a circular tank surrounded by water.

Since then, many analytical methods have been developed. They, however, were all carried out in the same fashion, which requires finding the solution of Laplace's equation that satisfies the boundary conditions.

Housner[7] derived satisfactory solutions by an approximate method which avoids partial differential equations and infinite series. First, he divided the dynamic fluid pressures into impulsive pressures and convective pressures, and then obtained the solution for each case. The formula of impulsive pressure p_i is given as follows:

$$p_i=\begin{cases}\sqrt{3}\,\rho h\left\{z/h+\frac{1}{2}(z/h)^2\right\}\ddot{u}_0\tanh(\sqrt{3}\,l/h) & :|z|<1.5L\\ \rho l\ddot{u}_0 & :|z|>1.5L,\end{cases} \qquad (3)$$

where ρ is the density of the fluid, $\ddot{u}_0$ is the tank acceleration, and h, l, L and z, which are shown in **Fig. 1**, are, respectively, the fluid depth, the half length of the sliced section, the half length of the tank, and the vertical coordinate positive upwards. In the case of a rectangular tank with the length of $2L$ and fluid depth of h, the impulsive pressure p_i is obtained by substituting of L into l in Eq. (3):

$$p_i=\begin{cases}\sqrt{3}\,\rho h\left\{z/h+\frac{1}{2}(z/h)^2\right\}\ddot{u}_0\tanh\left(\sqrt{3}\frac{L}{h}\right) & :|z|<1.5L\\ \rho L\ddot{u}_0 & :|z|>1.5L.\end{cases} \qquad (4)$$

In the case of a circular tank with a radius of r_0 and a fluid depth of h, the impulsive pressure at a point (r_0, θ) is also obtained by inserting of $r_0\cos\theta$ instead of l:

$$p_i=\begin{cases}\sqrt{3}\,\rho h\left\{z/h+\frac{1}{2}(z/h)^2\right\}\ddot{u}_0\tanh\left(\sqrt{3}\frac{r_0}{h}\cos\theta\right) & :|z|<1.5r_0\\ \rho r_0\ddot{u}_0\cos\theta & :|z|>1.5r_0.\end{cases} \qquad (5)$$

In the case of free oscillations of the fluid in the fundamental mode, which is produced by the movement of the tank wall, he obtained the convective pressure p_c in the fluid by

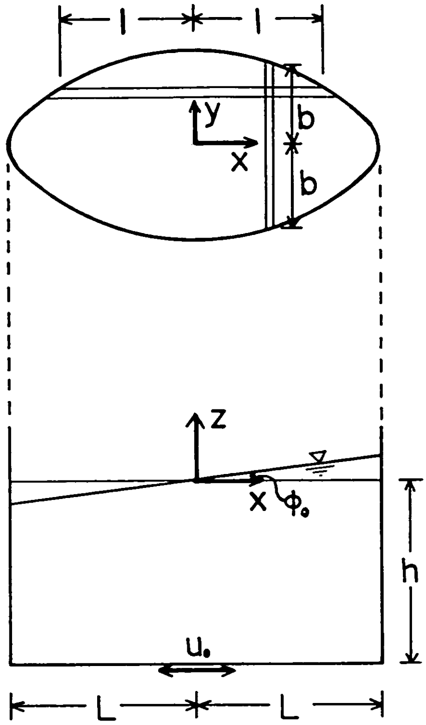

Fig. 1 Tank in Housner's Theory

$$p_c=\rho\phi_0 g\frac{I_z}{K}\left\{-\int\frac{Q}{b}dx+\frac{y^2}{2}\frac{b'}{b^2}Q\right\}\frac{\cosh\sqrt{\frac{I_z}{K}}(z+h)}{\cosh\sqrt{\frac{I_z}{K}}h}\sin\omega t, \tag{6 a}$$

where $$\left.\begin{aligned}&Q=\int_{-l}^{x}xbdx,\ b'=db/dx,\ \omega^2=g\sqrt{I_z/K}\tanh\sqrt{\frac{I_z}{K}}h,\\&I_z=\int_A x^2dA,\ \ K=2\int_{-L}^{L}\frac{1}{b}\left(\int_{-L}^{x}bxdx\right)^2\left(1+\frac{b'^2}{3}\right)dx,\end{aligned}\right\} \tag{6 b}$$

A is the horizontal area of the tank, ϕ_0 is the surface slope of the liquid, and x, y, z, and b are shown in **Fig. 1**. In the case of a rectangular tank with a length of $2L$, the convective pressure p_c is given as

$$p_c=\frac{5}{4}\rho\phi_0 gL\left\{\frac{x}{L}-\frac{1}{3}\left(\frac{x}{L}\right)^3\right\}\frac{\cosh\sqrt{\frac{5}{2}}\frac{1}{L}(z+h)}{\cosh\sqrt{\frac{5}{2}}\frac{h}{L}}\sin\omega t, \tag{7 a}$$

where $$\omega^2=\sqrt{\frac{5}{2}}\frac{g}{L}\tanh\sqrt{\frac{5}{2}}\frac{h}{L}. \tag{7 b}$$

In the case of a circular tank with a radius of r_0, the pressure p_c is given as follows:

$$p_c=\frac{9}{8}\rho\phi_0 gr_0\left\{\frac{x}{r_0}-\frac{1}{3}\left(\frac{x}{r_0}\right)^3-\frac{1}{4}\frac{x}{r_0}\left(\frac{z}{r_0}\right)^2\right\}\frac{\cosh\sqrt{\frac{27}{8}}\frac{z+h}{r_0}}{\cosh\sqrt{\frac{27}{8}}\frac{h}{r_0}}\sin\omega t, \tag{8 a}$$

where $$\omega^2=\sqrt{\frac{27}{8}\frac{g}{r_0}}\tanh\sqrt{\frac{27}{8}\frac{h}{r_0}}. \tag{8b}$$

Though many papers are published on the corresponding problems, the general earthquake proof design is founded on Housner's analysis. For example, the T.I.D. Report of U.S. AEC recommends the application of Housner's analysis to the design of tanks[8].

The sloshing phenomena where the fluid surface displacement resonates with a periodical external force of a period close to the natural frequency of the liquid, are very important in the design of tanks. Since the fluid surface displacement becomes so large during the sloshing that the linear analysis is no more valid. Therefore, nonlinear effects must be taken into account in the analysis of the sloshing phenomena. Chester[9] studied the shallow water case when the depth was very small, and showed that bores were formed in a model rectangular container. Faltinsen[10] dealt with the case of the water depth not being small when compared to the breadth of the rectangular tank.

With respect to the transient phenomena inside tanks, Sogabe and Shibata[11,12,13] studied them for circular structures, assuming an ideal fluid. For the transient state condition, they obtained the following velocity potential Φ at a point (r, θ):

$$\Phi=r_0\left[\sum_{i=1}^{\infty}\frac{2J_1(k_ir)\cosh k_i(h+z)}{(k_i^2r_0^2-1)J_1(k_ir_0)\cosh k_ih}v_i-\frac{r}{r_0}u_0\right]\cos\theta, \tag{9}$$

where r, θ and z are cylindrical coordinates, r_0 is the radius of the tank, k_i is the i-th solution of $J_1'(k_ir_0)=0$, $J_1(k_ir)$ is a Bessel function of the first kind, u_0 is the tank velocity, v_i is a solution of the following equation:

$$\ddot{v}_i+2\zeta_i\omega_i\dot{v}_i+\omega_i^2v_i=\ddot{u}_0+2\zeta_i\omega_i\dot{u}_0, \tag{10}$$

where $\omega_i^2=gk_i\tanh k_ih$, and ζ_i is a damping coefficient. From their experiments, they drew the conclusion that the value of ζ_i was very small and negligible. Using Eq. (9), they investigated the process of the growth of the fluid surface movements in resonance with the first mode frequency. As a result they presented a figure for the computation of the response magnification.

No other papers on the transient behabior of imcompressible fluids inside tanks could be found, although a few[14,15] dealt with the same problems for a compressible fluid.

In the case of a sea tank, two different fluids that completely fill the structure are usually oil and water. When such a tank is vibrated by an earthquake, internal waves are developed on the boundary surface between the liquids. Studies on those excited internal waves inside a sea tank are rare.

In the case of a circular tank, Ishikawa and Shiigai[16] studied them in a steady state condition. They concentrated their attention to the resonant internal waves of which period was close to the lowest natural frequency of the fluids, and obtained the solution for the internal waves of finite amplitude by perturbation method. They also carried out experiments, and concluded that the first approximate solution, which implies a linear solution, accurately represented the phenomena and that the true natural frequency was a little bit larger than the theoretical one. It is very interesting to notice that in their experiments, they observed cross waves traveling along the wall of the tank.

Sawamoto and Kato[17] analyzed the corresponding problem for a rectangular tank. The analytical method was quite the same as that of Shiigai and Ishikawa. In their experiments, they also observed cross waves: the causes of the wave development have not been made clear.

Although the above mentioned papers have dealt with the phenomena inside a tank vibrated by an earthquake, no papers have investigated the transient phenomena inside an undersea storage tank completely filled with two different liquids like oil and water. The results of field measurements of earthquake accelerations have clearly shown that an earthquake has two components of accelerations: one is horizontal and the other is vertical. Therefore, tanks must be shaken by an earthquake not only horizontally but also vertically. No papers, however, have discussed the effect of the vertical oscillation on the phenomena inside the tanks (either land or sea structures). The evaluation of the above two unsolved problems is important in order to estimate the proper seismic force to be used in the design of sea tanks.

3. Formulation of Dynamic Equations

It is assumed that a tank is completely filled with two fluids which have different densities ρ_{I} and ρ_{II} and that the two liquids have a clean smooth boundary surface between them and do not dissolve in each other. Furthermore, it is assumed that the liquids are imcompressible and are under no shear stress. Consequently, the liquids are taken as the ideal fluids.

If the liquid of density ρ_{I} in the upper layer is heavier than that of density ρ_{II} in the lower layer, the boundary surface becomes unstable and is gradually deformed by the sole action of a gravitational force. Finaly, the lighter fluid of density ρ_{II} occupies the upper layer. Therefore, it is natural to initially assume that the liquid of density ρ_{I} is lighter than that of density ρ_{II}.

As shown in **Fig. 2**, the origin of the coordinates (x, y, z) is fixed at the wall of the tank, and moves with it. Euler's dynamic equations of each liquid can be written as the vector expression:

$$\frac{\partial \boldsymbol{v}_{\mathrm{I}}}{\partial t}+(\boldsymbol{v}_{\mathrm{I}}\nabla)\boldsymbol{v}_{\mathrm{I}}=-\frac{1}{\rho_{\mathrm{I}}}\nabla p_{\mathrm{I}}-\boldsymbol{F}, \tag{11}$$

$$\frac{\partial \boldsymbol{v}_{\mathrm{II}}}{\partial t}+(\boldsymbol{v}_{\mathrm{II}}\nabla)\boldsymbol{v}_{\mathrm{II}}=-\frac{1}{\rho_{\mathrm{II}}}\nabla p_{\mathrm{II}}-\boldsymbol{F}, \tag{12}$$

where $\boldsymbol{v}$ and $\boldsymbol{F}$ represent the velocity vector of fluid particle and the external force vector exerted upon a fluid particle, respectively. They have components as follows:

$$\boldsymbol{v}_{\mathrm{I}}=(u_{\mathrm{I}}, v_{\mathrm{I}}, w_{\mathrm{I}}), \quad \boldsymbol{v}_{\mathrm{II}}=(u_{\mathrm{II}}, v_{\mathrm{II}}, w_{\mathrm{II}}), \tag{13}$$

$$\boldsymbol{F}=(f''_H(t)\cos\alpha, \quad f''_H(t)\sin\alpha, \quad g+f''_V(t)). \tag{14}$$

The fluid pressure is represented by p, and the suffixes I and II stand for the quantities related to the fluids of density ρ_{I} and ρ_{II}. In Eqs. (13) and (14), u, v and w, respectively, denote the velocity components to the axes of x, y and z. The functions $f_H(t)$ and $f_V(t)$ represent the horizontal displacement at an angle α to x-axis, and the vertical displacement. The gravitational acceleration is denoted by g. The symbol ∇ is vector operator:

$$\nabla=\frac{\partial}{\partial x}\boldsymbol{i}+\frac{\partial}{\partial y}\boldsymbol{j}+\frac{\partial}{\partial z}\boldsymbol{k}, \tag{15}$$

where $\boldsymbol{i}$, $\boldsymbol{j}$ and $\boldsymbol{k}$ are the unit vectors of the x, y and z axes, respectively.

We need other equations to solve Eqs. (11) and (12). They are the equation of mass continuity in each fluid, and are

$$\nabla\boldsymbol{v}_{\mathrm{I}}=0, \tag{16}$$

$$\nabla\boldsymbol{v}_{\mathrm{II}}=0. \tag{17}$$

Since boundary and initial conditions are necessary to obtain a unique solution, these conditions must be determined. On the boundary surface between the two liquids, two conditions must be satisfied: one is that the pressure in the upper layer must equal that in the lower layer, and the other is that the boundary surface displacement calculated in the upper layer must be equal to that calculated in the lower layer. The former condition is expressed in the

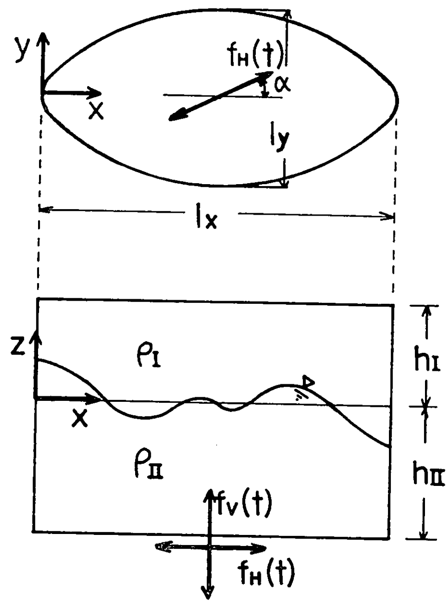

Fig. 2 Schematic Drawing of a Sea Tank

following equation:

$$p_{\mathrm{I}}|_{z=\zeta}=p_{\mathrm{II}}|_{z=\zeta}, \tag{18}$$

where ζ is the displacement of the boundary surface from its still position. The latter condition can be obtained as follows:

$$\begin{aligned}\frac{\partial\zeta}{\partial t}&=\omega_{\mathrm{I}}|_{z=\zeta}-u_{\mathrm{I}}|_{z=\zeta}\frac{\partial\zeta}{\partial x}-v_{\mathrm{I}}|_{z=\zeta}\frac{\partial\zeta}{\partial y}\\&=\omega_{\mathrm{II}}|_{z=\zeta}-u_{\mathrm{II}}|_{z=\zeta}\frac{\partial\zeta}{\partial x}-v_{\mathrm{II}}|_{z=\zeta}\frac{\partial\zeta}{\partial y}.\end{aligned} \tag{19}$$

On the rigid boundaries like side walls, bottom and ceiling of the tank, the velocity must satisfy the condition that its normal component to the boundary vanishes on the moving coordinates. This condition can be expressed as follows:

$$\boldsymbol{n}\cdot\boldsymbol{v}_{\mathrm{I}}=0 \quad , \quad \boldsymbol{n}\cdot\boldsymbol{v}_{\mathrm{II}}=0, \tag{20}$$

where $\boldsymbol{n}$ is the unit vector along the normal to the rigid boundary.

In addition to the above conditions, the initial conditions given by the following equations are necessary:

$$\boldsymbol{v}_{\mathrm{I}}|_{t\leq 0}=0, \tag{21}$$

$$\boldsymbol{v}_{\mathrm{II}}|_{t\leq 0}=0. \tag{22}$$

When $\boldsymbol{r}$ represents the displacement vector of a fluid particle, it can be expressed as

$$\boldsymbol{r}_{\mathrm{I}}=\int_0^t\boldsymbol{v}_{\mathrm{I}}dt, \tag{23}$$

$$\boldsymbol{r}_{\mathrm{II}}=\int_0^t\boldsymbol{v}_{\mathrm{II}}dt. \tag{24}$$

Equations (23) and (24) mean that a fluid particle keeps its still position until the tank starts to oscillate.

We can obtain the unique solution if we solve Eqs. (11), (12), (16) and (17) under the boundary conditions given by Eqs. (18) to (20) and the initial conditions of Eqs. (21) to (24).

4. Linearization of Equations

Some of the equations of motion, of continuity equations of fluid mass, and of boundary and initial conditions, which are given in 3, include nonlinear terms. Since it is very difficult to solve these equations under these conditions, the linearization of the equations will be investigated in this chapter.

In problems such as forced oscillation, the most influential quantities are the amplitude and the period of the tank movement, the size of the tank, the thickness of the lower and upper layers, and the densities of the two liquids. The following quantities are used in order to make all of the quantities nondimensionalized.

For the tank displacement, the mean amplitude B_H and the mean period T_H of the horizontal displcement are used. With respect to the size of the tank, the lengthes of l_x and l_y are used. As for the thickness of the layers, each thickness in the still state is used and represented by h_{I} or h_{II}. The densities ρ_{I} and ρ_{II} are used.

By using these representative quantities, all quantities in question are nondimensionalized as follows:

$$\left.\begin{array}{l}
x=l_x\tilde{x},\ \ y=l_y\tilde{y},\ \ z=\begin{cases}h_{\mathrm{I}}\tilde{z}\ \text{(in upper layer)}\\ h_{\mathrm{II}}\tilde{z}\ \text{(in lower layer)},\end{cases}\\
u_{\mathrm{I}}=B_H\tilde{u}_{\mathrm{I}}/T_H,\quad v_{\mathrm{I}}=B_H\tilde{v}_{\mathrm{I}}/T_H,\quad w_{\mathrm{I}}=B_H\tilde{w}_{\mathrm{I}}/T_H,\\
u_{\mathrm{II}}=B_H\tilde{u}_{\mathrm{II}}/T_H,\quad v_{\mathrm{II}}=B_H\tilde{v}_{\mathrm{II}}/T_H,\quad w_{\mathrm{II}}=B_H\tilde{w}_{\mathrm{II}}/T_H,\\
f_H''(t)=B_H\tilde{f}_H''/T_H^2,\qquad f_V''(t)=B_H\tilde{f}_V''/T_H^2,\\
p_{\mathrm{I}}=\rho_{\mathrm{I}}h_{\mathrm{I}}B_H\tilde{p}_{\mathrm{I}}/T_H^2,\qquad p_{\mathrm{II}}=\rho_{\mathrm{II}}h_{\mathrm{II}}B_H\tilde{p}_{\mathrm{II}}/T_H^2,\\
\zeta=B_H\tilde{\zeta},\qquad t=T_H\tilde{t},\qquad g=B_H\tilde{g}/T_H^2,
\end{array}\right\} \tag{25}$$

where the swung bar refers to nondimensional quantities.

Substituting Eq. (25) into Eqs. (11) and (12), which include nonlinear terms, gives the following nondimensional equations:

$$\left.\begin{array}{l}
\dfrac{\partial\tilde{u}_{\mathrm{I}}}{\partial t}+\dfrac{B_H}{l_x}\tilde{u}_{\mathrm{I}}\dfrac{\partial\tilde{u}_{\mathrm{I}}}{\partial\tilde{x}}+\dfrac{B_H}{l_y}\tilde{v}_{\mathrm{I}}\dfrac{\partial\tilde{u}_{\mathrm{I}}}{\partial\tilde{y}}+\dfrac{B_H}{h_{\mathrm{I}}}\tilde{w}_{\mathrm{I}}\dfrac{\partial\tilde{u}_{\mathrm{I}}}{\partial\tilde{z}}=-\dfrac{h_{\mathrm{I}}}{l_x}\dfrac{\partial\tilde{p}_{\mathrm{I}}}{\partial\tilde{x}}-\tilde{f}_H''\cos\alpha,\\
\dfrac{\partial\tilde{v}_{\mathrm{I}}}{\partial t}+\dfrac{B_H}{l_x}\tilde{u}_{\mathrm{I}}\dfrac{\partial\tilde{v}_{\mathrm{I}}}{\partial\tilde{x}}+\dfrac{B_H}{l_y}\tilde{v}_{\mathrm{I}}\dfrac{\partial\tilde{v}_{\mathrm{I}}}{\partial\tilde{y}}+\dfrac{B_H}{h_{\mathrm{I}}}\tilde{w}_{\mathrm{I}}\dfrac{2\tilde{v}_{\mathrm{I}}}{\partial\tilde{z}}=-\dfrac{h_{\mathrm{I}}}{l_y}\dfrac{\partial\tilde{p}_{\mathrm{I}}}{\partial\tilde{y}}-\tilde{f}_H''\sin\alpha,\\
\dfrac{\partial\tilde{w}_{\mathrm{I}}}{\partial t}+\dfrac{B_H}{l_x}\tilde{u}_{\mathrm{I}}\dfrac{\partial\tilde{w}_{\mathrm{I}}}{\partial\tilde{x}}+\dfrac{B_H}{l_y}\tilde{v}_{\mathrm{I}}\dfrac{\partial\tilde{w}_{\mathrm{I}}}{\partial\tilde{y}}+\dfrac{B_H}{h_{\mathrm{I}}}\tilde{w}_{\mathrm{I}}\dfrac{\partial\tilde{w}_{\mathrm{I}}}{\partial\tilde{z}}=-\dfrac{\partial\tilde{p}_{\mathrm{I}}}{\partial\tilde{z}}-\tilde{g}-\tilde{f}_V''.
\end{array}\right\} \tag{26}$$

When the suffix I in Eq. (26) is changed to II, Eq. (26) becomes the nondimensional dynamic fluid equations of the lower layer. To linearize each equation of Eq. (26), the effect of the nonlinear terms (the second to fourth terms in the left hand side) must be small enough in comparison with that of the linear terms to be omitted. Therefore, the following conditions are inferred:

$$\frac{B_H}{l_x}\ll 1,\quad \frac{B_H}{l_y}\ll 1,\quad \frac{B_H}{h_{\mathrm{I}}}\ll 1,\quad \frac{B_H}{h_{\mathrm{II}}}\ll 1. \tag{27}$$

From Eq. (27), it is seen that the amplitude of the tank displacement must be much smaller than the size of the tank and the thickness of each fluid layer.

By substituting Eq. (25) into Eq. (19), the following nondimensional equation of the boundary surface displacement can be obtained:

$$\frac{\partial\tilde{\zeta}}{\partial\tilde{t}}=\tilde{w}_{\mathrm{I}}\Big|_{\tilde{z}=B_H\tilde{\zeta}/h_{\mathrm{I}}}-\frac{B_H}{l_x}\tilde{u}_{\mathrm{I}}\Big|_{\tilde{z}=\frac{B_H}{h_{\mathrm{I}}}\tilde{\zeta}}\frac{\partial\tilde{\zeta}}{\partial\tilde{x}}-\frac{B_H}{l_y}\tilde{v}_{\mathrm{I}}\Big|_{\tilde{z}=\frac{B_H}{h_{\mathrm{I}}}\tilde{\zeta}}\frac{\partial\tilde{\zeta}}{\partial\tilde{y}}. \tag{28}$$

If $\tilde{z}=B_H\tilde{\zeta}/h_{\mathrm{I}}$ is small, each term of the right hand side can be developed around $\tilde{z}=0$ by Taylor's expansion as such:

$$\begin{aligned}\frac{\partial\tilde{\zeta}}{\partial\tilde{t}}=&\,\tilde{w}_{\mathrm{I}}\Big|_{\tilde{z}=0}+\frac{B_H}{h_{\mathrm{I}}}\tilde{\zeta}\frac{\partial\tilde{w}_{\mathrm{I}}}{\partial\tilde{z}}\Big|_{\tilde{z}=0}+\cdots\cdots\cdots\\&-\frac{B_H}{l_x}\tilde{u}_{\mathrm{I}}\Big|_{\tilde{z}=0}\frac{\partial\tilde{\zeta}}{\partial\tilde{x}}-\frac{B_H^2}{l_xh_{\mathrm{I}}}\tilde{\zeta}\frac{\partial\tilde{u}_{\mathrm{I}}}{\partial\tilde{z}}\Big|_{\tilde{z}=0}\frac{\partial\tilde{\zeta}}{\partial\tilde{x}}\cdots\cdots\cdots\cdots\\&-\frac{B_H}{l_y}\tilde{v}_{\mathrm{I}}\Big|_{\tilde{z}=0}\frac{\partial\tilde{\zeta}}{\partial\tilde{y}}-\frac{B_H^2}{l_yh_{\mathrm{I}}}\tilde{\zeta}\frac{\partial\tilde{v}_{\mathrm{I}}}{\partial\tilde{z}}\Big|_{\tilde{z}=0}\frac{\partial\tilde{\zeta}}{\partial\tilde{y}}-\cdots\cdots\cdots\cdots.\end{aligned} \tag{29}$$

Applying of the linearization conditions of Eq. (27), Eq. (29) is easily linearized as follows:

$$\frac{\partial\tilde{\zeta}}{\partial\tilde{t}}=\tilde{w}_{\mathrm{I}}\Big|_{\tilde{z}=0}. \tag{30}$$

With repect to the liquid of density ρ_{II}, a similar equation to Eq. (30) is derived as follows:

$$\frac{\partial\tilde{\zeta}}{\partial\tilde{t}}=\tilde{w}_{\mathrm{II}}\Big|_{\tilde{z}=0}. \tag{31}$$

By combining Eqs. (30) and (31), the following relation can be obtained:

$$\tilde{w}_{\mathrm{I}}|_{\tilde{z}=0}=\tilde{w}_{\mathrm{II}}|_{\tilde{z}=0}. \tag{32}$$

If we accept the linearization condition of Eq. (27), we can derive the pressure p_{I} on the fluid boundary surface from the third equation of Eq. (26) as

$$\tilde{p}_{\mathrm{I}}\Big|_{\tilde{z}=\frac{B_H}{h_{\mathrm{I}}}\tilde{\zeta}}-\tilde{p}_{\mathrm{I}}\Big|_{\tilde{z}=0}=-\int_0^{\tilde{z}=\frac{B_H}{h_{\mathrm{I}}}\tilde{\zeta}}\frac{\partial\tilde{w}_{\mathrm{I}}}{\partial\tilde{t}}d\tilde{z}-\frac{B_H}{h_{\mathrm{I}}}\tilde{\zeta}\tilde{g}-\frac{B_H}{h_{\mathrm{I}}}\tilde{\zeta}\tilde{f}_V''. \tag{33}$$

Considering the quantity of $B_H\tilde{\zeta}/h_{\mathrm{I}}$ to be small, Eq. (33) is reduced to

$$\tilde{p}_{\mathrm{I}}\Big|_{\tilde{z}=\frac{B_H}{h_{\mathrm{I}}}\tilde{\zeta}}-\tilde{p}_{\mathrm{I}}\Big|_{\tilde{z}=0}=-\frac{B_H}{h_{\mathrm{I}}}\tilde{\zeta}\left(\tilde{g}+\tilde{f}_V''+\frac{\partial\tilde{w}_{\mathrm{I}}}{\partial\tilde{t}}\Big|_{\tilde{z}=0}\right). \tag{34}$$

In the same way, we can derive the pressure p_{II} as

$$\tilde{p}_{\mathrm{II}}\Big|_{\tilde{z}=\frac{B_H}{h_{\mathrm{II}}}\tilde{\zeta}}-\tilde{p}_{\mathrm{II}}\Big|_{\tilde{z}=0}=-\frac{B_H}{h_{\mathrm{II}}}\tilde{\zeta}\left(\tilde{g}+\tilde{f}_V''+\frac{\partial\tilde{w}_{\mathrm{II}}}{\partial\tilde{t}}\Big|_{\tilde{z}=0}\right), \tag{35}$$

Since $p_{\mathrm{II}}|_{z=\zeta}$ is equal to $p_{\mathrm{I}}|_{z=\zeta}$ on the boundary surface from Eq. (18),

$$\tilde{p}_{\mathrm{II}}\Big|_{\tilde{z}=\frac{B_H}{h_{\mathrm{II}}}\tilde{\zeta}}=\frac{\rho_{\mathrm{I}}h_{\mathrm{I}}}{\rho_{\mathrm{II}}h_{\mathrm{II}}}\tilde{p}_{\mathrm{I}}\Big|_{\tilde{z}=\frac{B_H}{h_{\mathrm{I}}}\tilde{\zeta}}, \tag{36}$$

and from Eqs. (34), (35) and (36) we get

$$\tilde{p}_{\mathrm{II}}\Big|_{\tilde{z}=0}=\frac{\rho_{\mathrm{I}}h_{\mathrm{I}}}{\rho_{\mathrm{II}}h_{\mathrm{II}}}\tilde{p}_{\mathrm{I}}\Big|_{\tilde{z}=0}+\frac{B_H}{h_{\mathrm{II}}}\tilde{\zeta}\left(\tilde{g}+\tilde{f}_V''+\frac{\partial\tilde{w}_{\mathrm{II}}}{\partial\tilde{t}}\Big|_{\tilde{z}=0}\right)-\frac{\rho_{\mathrm{I}}}{\rho_{\mathrm{II}}}\frac{B_H}{h_{\mathrm{II}}}\tilde{\zeta}\left(\tilde{g}+\tilde{f}_V''+\frac{\partial\tilde{w}_{\mathrm{I}}}{\partial\tilde{t}}\Big|_{\tilde{z}=0}\right). \tag{37}$$

In the relation of Eq. (32), Eq. (37) is more simplified as follows:

$$\tilde{p}_{\mathrm{II}}\Big|_{\tilde{z}=0}=\frac{\rho_{\mathrm{I}}h_{\mathrm{I}}}{\rho_{\mathrm{II}}h_{\mathrm{II}}}\tilde{p}_{\mathrm{I}}\Big|_{\tilde{z}=0}+\frac{B_H}{h_{\mathrm{II}}}\tilde{\zeta}\left(1-\frac{\rho_{\mathrm{I}}}{\rho_{\mathrm{II}}}\right)\left(\tilde{g}+\tilde{f}''_V+\frac{\partial\tilde{w}_{\mathrm{II}}}{\partial\tilde{t}}\Big|_{\tilde{z}=0}\right). \tag{38}$$

If

$$\left|\frac{\partial\tilde{w}_{\mathrm{II}}}{\partial\tilde{t}}\Big|_{\tilde{z}=0}\right|/|\tilde{g}+\tilde{f}''_V|\ll 1, \tag{39}$$

then Eq. (38) becomes linear, and is written as

$$\tilde{p}_{\mathrm{II}}\Big|_{\tilde{z}=0}=\frac{\rho_{\mathrm{I}}h_{\mathrm{I}}}{\rho_{\mathrm{II}}h_{\mathrm{II}}}\tilde{p}_{\mathrm{I}}\Big|_{\tilde{z}=0}+\frac{B_H}{h_{\mathrm{II}}}\tilde{\zeta}\left(\tilde{g}+\tilde{f}''_V\right)\left(1-\frac{\rho_{\mathrm{I}}}{\rho_{\mathrm{II}}}\right). \tag{40}$$

When Eq. (39) is rewritten in dimensional form, it becomes

$$\left|\frac{\partial w_{\mathrm{I}}}{\partial t}\Big|_{z=0}\right|=\left|\frac{\partial w_{\mathrm{II}}}{\partial t}\Big|_{z=0}\right|\ll\left|g+f''_V(t)\right|. \tag{41}$$

By the relation of Eq. (31), it is reduced to

$$\left|\frac{\partial^2\zeta}{\partial t^2}\right|\ll\left|g+f''_V(t)\right|. \tag{42}$$

Since the other equations like those of the continuity of mass, and of the boundry and the initial conditions, do not include nonlinear terms, it is not necessary to carry out their nondimensional analysis in order to obtain the condition for the linearlization. After all, the conditions of the linearlization are given by Eqs. (27) and (39).

Since the amplitudes of tank displacements due to an earthquake is very small compared with the size of a tank, the conditions of Eq. (27) are supposed to be satisfied. The condition of Eq. (39), however, will have to be verified by field observation of vertical acceleration of earthquakes and measurements of the fluid boundary surface displacements.

5. Derivation of Basic Differential Equations

5.1 Rectangular Tanks

By nondimensional analysis, all equations can be linearized if Eqs. (27) and (39) are satisfied.

The origin of the coordinates (x, y, z) is fixed at a corner of the tank, as shown in **Fig. 3**. The linearized dynamic equations are written for each fluid as follows:

$$\left.\begin{aligned}\frac{\partial u_{\mathrm{I}}}{\partial t}&=-\frac{\partial p_{\mathrm{I}}}{\rho_{\mathrm{I}}\partial x}-f''_H(t)\cos\alpha,\\ \frac{\partial v_{\mathrm{I}}}{\partial t}&=-\frac{\partial p_{\mathrm{I}}}{\rho_{\mathrm{I}}\partial y}-f''_H(t)\sin\alpha,\\ \frac{\partial w_{\mathrm{I}}}{\partial t}&=-\frac{\partial p_{\mathrm{I}}}{\rho_{\mathrm{I}}\partial z}-g-f''_V(t),\end{aligned}\right\} \tag{43}$$

$$\left.\begin{aligned}\frac{\partial u_{\mathrm{II}}}{\partial t}&=-\frac{\partial p_{\mathrm{II}}}{\rho_{\mathrm{II}}\partial x}-f''_H(t)\cos\alpha,\\ \frac{\partial v_{\mathrm{II}}}{\partial t}&=-\frac{\partial p_{\mathrm{II}}}{\rho_{\mathrm{II}}\partial y}-f''_H(t)\sin\alpha,\\ \frac{\partial w_{\mathrm{II}}}{\partial t}&=-\frac{\partial p_{\mathrm{II}}}{\rho_{\mathrm{II}}\partial z}-g-f''_V(t).\end{aligned}\right\} \tag{44}$$

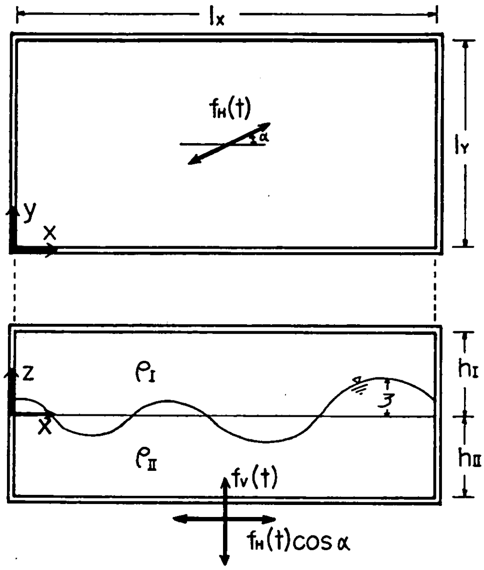

Fig. 3 Rectangular Tank

The continuity equations of fluid mass of Eqs. (16) and (17) is rewritten in the expressions with the velocity components as

$$\frac{\partial u_{\rm I}}{\partial x}+\frac{\partial v_{\rm I}}{\partial y}+\frac{\partial w_{\rm I}}{\partial z}=0, \tag{45}$$

$$\frac{\partial u_{\rm II}}{\partial x}+\frac{\partial v_{\rm II}}{\partial y}+\frac{\partial w_{\rm II}}{\partial z}=0. \tag{46}$$

From Eqs. (30), (31) and (40), the conditions of the boundary surface between the two liquids can be written in the following linearized forms:

$$\frac{\partial \zeta}{\partial t}=w_{\rm I}\Big|_{z=0}=w_{\rm II}\Big|_{z=0}, \tag{47}$$

$$p_{\rm II}|_{z=0}=p_{\rm I}|_{z=0}+(\rho_{\rm II}-\rho_{\rm I})\zeta(g+f''_V(t)). \tag{48}$$

The boundary conditions for the rigid boundary are universally expressed in Eq. (20), but in the case of a rectangular tank with a longitudinal length l_x and a width l_y, it is more convenient to divide them into each condition, like on side walls at $x=0$ or l_x, and $y=0$ or l_y, on the bottom at $z=-h_{\rm II}$, or on the ceilling at $z=h_{\rm I}$ thus:

$$u_{\rm I}|_{x=0,l_x}=0,\quad u_{\rm II}|_{x=0,l_x}=0, \tag{49}$$

$$v_{\rm I}|_{y=0,l_y}=0,\quad v_{\rm II}|_{y=0,l_y}=0, \tag{50}$$

$$w_{\rm I}|_{z=h_{\rm I}}=0,\quad w_{\rm II}|_{z=-h_{\rm II}}=0. \tag{51}$$

The initial conditions are written as follows:

$$\left.\begin{array}{ll} u_{\rm I}|_{t\le 0}=0, & u_{\rm II}|_{t\le 0}=0,\\ v_{\rm I}|_{t\le 0}=0, & v_{\rm II}|_{t\le 0}=0,\\ w_{\rm I}|_{t\le 0}=0, & w_{\rm II}|_{t\le 0}=0. \end{array}\right\} \tag{52}$$

The displacement (X, Y, Z) of a fluid particle in the x, y and z-directions are expressed with respect to each layer as follows:

$$\left.\begin{aligned} X_{\rm I}&=\int_0^t u_{\rm I}dt\ ,\quad X_{\rm II}=\int_0^t u_{\rm II}dt,\\ Y_{\rm I}&=\int_0^t v_{\rm I}dt\ ,\quad Y_{\rm II}=\int_0^t v_{\rm II}dt,\\ Z_{\rm I}&=\int_0^t w_{\rm I}dt\ ,\quad Z_{\rm II}=\int_0^t w_{\rm II}dt. \end{aligned}\right\} \tag{53}$$

Since a fluid particle on the side wall moves with the tank displacement, there occur no relative displacements along the normal to the wall. Therefore, the boundary conditions of the fluid particle displacement on the rigid boundary are reduced to

$$\left.\begin{aligned} &X_{\rm I}\,|_{x=0,l_x}=0,\\ &X_{\rm II}\,|_{x=0,l_x}=0,\\ &Y_{\rm I}\,|_{y=0,l_y}=0,\\ &Y_{\rm II}\,|_{y=0,l_y}=0,\\ &Z_{\rm I}\,|_{z=h{\rm I}}\ =0,\\ &Z_{\rm II}\,|_{z=-h{\rm II}}=0. \end{aligned}\right\} \tag{54}$$

Referring to Eq. (54), $X_{\rm I}$, $X_{\rm II}$, $Y_{\rm I}$ and $Y_{\rm II}$ may be represented as follows:

$$\left.\begin{aligned} X_{\rm I}&=\sum_{n=0}^{\infty}A_{{\rm I}n}(t)\,B_{{\rm I}n}(z)\sin\frac{n\pi}{l_x}x,\\ X_{\rm II}&=\sum_{n=0}^{\infty}A_{{\rm II}n}(t)\,B_{{\rm II}n}(z)\sin\frac{n\pi}{l_x}x,\\ Y_{\rm I}&=\sum_{n=0}^{\infty}C_{{\rm I}n}(t)\,D_{{\rm I}n}(z)\sin\frac{n\pi}{l_y}y,\\ Y_{\rm II}&=\sum_{n=0}^{\infty}C_{{\rm II}n}(t)\,D_{{\rm II}n}(z)\sin\frac{n\pi}{l_y}y, \end{aligned}\right\} \tag{55}$$

where $A_{{\rm I}n}(t)$, $A_{{\rm II}n}(t)$, $C_{{\rm I}n}(t)$ and $C_{{\rm II}n}(t)$ are functions of t only, and $B_{{\rm I}n}(z)$, $B_{{\rm II}n}(z)$, $D_{{\rm I}n}(z)$ and $D_{{\rm II}n}(z)$ are functions of z only.
From Eq. (53), $u_{\rm I}$, $u_{\rm II}$, $v_{\rm I}$ and $v_{\rm II}$ can be easily derived as

$$\left.\begin{aligned} u_{\rm I}&=\sum_{n=0}^{\infty}A'_{{\rm I}n}(t)\,B_{{\rm I}n}(z)\sin\frac{n\pi}{l_x}x,\\ u_{\rm II}&=\sum_{n=0}^{\infty}A'_{{\rm II}n}(t)\,B_{{\rm II}n}(z)\sin\frac{n\pi}{l_x}x,\\ v_{\rm I}&=\sum_{n=0}^{\infty}C'_{{\rm I}n}(t)\,D_{{\rm I}n}(z)\sin\frac{n\pi}{l_y}y,\\ v_{\rm II}&=\sum_{n=0}^{\infty}C'_{{\rm II}n}(t)\,D_{{\rm II}n}(z)\sin\frac{n\pi}{l_y}y. \end{aligned}\right\} \tag{56}$$

The velocities $u_{\rm I}$, $u_{\rm II}$, $v_{\rm I}$ and $v_{\rm II}$ in Eq. (56) obviously satisfy the boundary conditions of Eqs. (49) and (50). By substituting Eq. (56) into Eqs. (45) and (46) and integrating with repect to z under the condition of Eq. (51), $w_{\rm I}$ and $w_{\rm II}$ can be obtained as follows:

$$\begin{aligned} w_{\rm I}=&-\sum_{n=0}^{\infty}\frac{n\pi}{l_x}A'_{{\rm I}n}(t)\cos\frac{n\pi}{l_x}x\int_{h{\rm I}}^{z}B_{{\rm I}n}(z)dz\\ &-\sum_{n=0}^{\infty}\frac{n\pi}{l_y}C'_{{\rm I}n}(t)\cos\frac{n\pi}{l_y}y\int_{h{\rm I}}^{z}D_{{\rm I}n}(z)dz, \end{aligned} \tag{57}$$

$$w_{\mathrm{II}}=-\sum_{n=0}^{\infty}\frac{n\pi}{l_x}A'_{\mathrm{II}n}(t)\cos\frac{n\pi}{l_x}x\int_{-h_{\mathrm{II}}}^{z}B_{\mathrm{II}n}(z)dz$$
$$-\sum_{n=0}^{\infty}\frac{n\pi}{l_y}C'_{\mathrm{II}n}(t)\cos\frac{n\pi}{l_y}y\int_{-h_{\mathrm{II}}}^{z}D_{\mathrm{II}n}(z)dz. \tag{58}$$

From Eq. (47), ζ and the relations between $A_{\mathrm{I}n}(t)$ and $A_{\mathrm{II}n}(t)$ and between $C_{\mathrm{I}n}(t)$ and $C_{\mathrm{II}n}(t)$ can now be derived as follows:

$$\zeta=-\sum_{n=0}^{\infty}\frac{n\pi}{l_x}A_{\mathrm{II}n}(t)\cos\frac{n\pi}{l_x}x\int_{-h_{\mathrm{II}}}^{0}B_{\mathrm{II}n}(z)dz$$
$$-\sum_{n=0}^{\infty}\frac{n\pi}{l_y}C_{\mathrm{II}n}(t)\cos\frac{n\pi}{l_y}y\int_{-h_{\mathrm{II}}}^{0}D_{\mathrm{II}n}(z)dz \tag{59}$$

$$\left.\begin{aligned}A_{\mathrm{I}n}(t)&=A_{\mathrm{II}n}(t)\int_{-h_{\mathrm{II}}}^{0}B_{\mathrm{II}n}(z)dz\Big/\int_{h_{\mathrm{I}}}^{0}B_{\mathrm{I}n}(z)dz\\ C_{\mathrm{I}n}(t)&=C_{\mathrm{II}n}(t)\int_{-h_{\mathrm{II}}}^{0}D_{\mathrm{II}n}(z)dz\Big/\int_{h_{\mathrm{I}}}^{0}D_{\mathrm{I}n}(z)dz\end{aligned}\right\} \tag{60}$$

Furthermore, p_{I} and p_{II} can be given by substituting Eqs. (57) and (58) into the third equations of Eqs. (43) and (44), respectively, and integrating them with respect to z. They then become

$$p_{\mathrm{I}}=p_{\mathrm{I}}|_{z=0}-\rho_{\mathrm{I}}gz-\rho_{\mathrm{I}}f''_V(t)z+\rho_{\mathrm{I}}\sum_{n=0}^{\infty}\Big[\frac{n\pi}{l_x}A''_{\mathrm{I}n}(t)\cos\frac{n\pi}{l_x}x$$
$$\times\int_0^z\int_{h_{\mathrm{I}}}^{\eta}B_{\mathrm{I}n}(\xi)d\xi d\eta+\frac{n\pi}{l_y}C''_{\mathrm{I}n}(t)\cos\frac{n\pi}{l_y}y\int_0^z\int_{h_{\mathrm{I}}}^{\eta}D_{\mathrm{I}n}(\xi)d\xi d\eta\Big], \tag{61}$$

and

$$p_{\mathrm{II}}=p_{\mathrm{II}}|_{z=0}-\rho_{\mathrm{II}}gz-\rho_{\mathrm{II}}f''_V(t)z+\rho_{\mathrm{II}}\sum_{n=0}^{\infty}\Big[\frac{n\pi}{l_x}A''_{\mathrm{II}n}(t)\cos\frac{n\pi}{l_x}x$$
$$\times\int_0^z\int_{-h_{\mathrm{II}}}^{\eta}B_{\mathrm{II}}(\xi)d\xi d\eta+\frac{n\pi}{l_y}C''_{\mathrm{II}n}(t)\cos\frac{n\pi}{l_y}y\int_0^z\int_{-h_{\mathrm{II}}}^{\eta}D_{\mathrm{II}n}(\xi)d\xi d\eta\Big], \tag{62}$$

where $p_{\mathrm{I}}|_{z=0}$ and $p_{\mathrm{II}}|_{z=0}$ are integral constants.

If u_{I} and v_{I} in Eq. (56) and p_{I} in Eq. (61) are substituted into the first and the second equations of Eq. (43), they yield

$$\sum_{n=0}^{\infty}A''_{\mathrm{I}n}(t)B_{\mathrm{I}n}(z)\sin\frac{n\pi}{l_x}x$$
$$=-\frac{1}{\rho_{\mathrm{I}}}\frac{\partial p_{\mathrm{I}}|_{z=0}}{\partial x}+\sum_{n=0}^{\infty}\Big[\Big(\frac{n\pi}{l_x}\Big)^2A''_{\mathrm{I}n}(t)\sin\frac{n\pi}{l_x}x\int_0^z\int_{h_{\mathrm{I}}}^{\eta}B_{\mathrm{I}n}(\xi)d\xi d\eta\Big]$$
$$-f''_H(t)\cos\alpha, \tag{63}$$

$$\sum_{n=0}^{\infty}C''_{\mathrm{I}n}(t)D_{\mathrm{I}n}(z)\sin\frac{n\pi}{l_y}y$$
$$=-\frac{1}{\rho_{\mathrm{I}}}\frac{\partial p_{\mathrm{I}}|_{z=0}}{\rho y}+\sum_{n=0}^{\infty}\Big[\Big(\frac{n\pi}{l_y}\Big)^2C''_{\mathrm{I}n}(t)\sin\frac{n\pi}{l_y}y\int_0^z\int_{h_{\mathrm{I}}}^{\eta}D_{\mathrm{I}n}(\xi)d\xi d\eta\Big]$$
$$-f''_H(t)\sin\alpha. \tag{64}$$

Differentiation of Eqs. (63) and (64) by z gives

$$\sum_{n=0}^{\infty}A''_{\mathrm{I}n}(t)B'_{\mathrm{I}n}(z)\sin\frac{n\pi}{l_x}x$$
$$=\sum_{n=0}^{\infty}\Big(\frac{n\pi}{l_x}\Big)^2A''_{\mathrm{I}n}(t)\sin\frac{n\pi}{l_x}x\int_{h_{\mathrm{I}}}^{z}B_{\mathrm{I}n}(z)dz, \tag{65}$$

$$\sum_{n=0}^{\infty} C''_{\mathrm{I}n}(t) D'_{\mathrm{I}n}(z) \sin\frac{n\pi}{l_y} y$$
$$=\sum_{n=0}^{\infty}\left(\frac{n\pi}{l_y}\right)^2 C''_{\mathrm{I}n}(t)\sin\frac{n\pi}{l_y} y\int_{h\mathrm{I}}^{z} D_{\mathrm{I}n}(z)\,dz. \tag{66}$$

Multipliying Eqs. (65) and (66) by $\sin(n\pi x/l_x)$ and $\sin(n\pi y/l_y)$ and then integrating them with respect to x and y from 0 to l_x and l_y respectively, we can obtain

$$\left.\begin{aligned} B'_{\mathrm{I}n}(z)&=\left(\frac{n\pi}{l_x}\right)^2\int_{h\mathrm{I}}^{z} B_{\mathrm{I}n}(z)\,dz,\\ D'_{\mathrm{I}n}(z)&=\left(\frac{n\pi}{l_y}\right)^2\int_{h\mathrm{I}}^{z} D_{\mathrm{I}n}(z)\,dz.\end{aligned}\right\} \tag{67}$$

The solutions of Eq. (67) can easily be obtained as follows:

$$\left.\begin{aligned} B_{\mathrm{I}n}(z)&=\cosh\frac{n\pi}{l_x}(z-h_{\mathrm{I}}),\\ D_{\mathrm{I}n}(z)&=\cosh\frac{n\pi}{l_y}(z-h_{\mathrm{I}}).\end{aligned}\right\} \tag{68}$$

The respective substitution of $B_{\mathrm{I}n}(z)$ and $D_{\mathrm{I}n}(z)$ in Eq. (68) into Eqs. (63) and (64) gives

$$\sum_{n=0}^{\infty} A''_{\mathrm{I}n}(t)\cosh\frac{n\pi}{l_x}h_{\mathrm{I}}\sin\frac{n\pi}{l_x}x=\frac{\partial p_{\mathrm{I}}|_{z=0}}{\rho_{\mathrm{I}}\partial x}-f''_H(t)\cos\alpha, \tag{69}$$

$$\sum_{n=0}^{\infty} C''_{\mathrm{I}n}(t)\cosh\frac{n\pi}{l_y}h_{\mathrm{I}}\sin\frac{n\pi}{l_y}y=-\frac{\partial p_{\mathrm{I}}|_{z=0}}{\rho_{\mathrm{I}}\partial y}-f''_H(t)\sin\alpha. \tag{70}$$

Substituting Eq. (62) and u_{II} and v_{II} of Eq. (56) into the first and the second equations of Eq. (44) gives

$$\sum_{n=0}^{\infty} A''_{\mathrm{II}n}(t) B_{\mathrm{II}n}(z)\sin\frac{n\pi}{l_x}x$$
$$=\frac{\partial p_{\mathrm{II}}|_{z=0}}{\rho_{\mathrm{II}}\partial x}+\sum_{n=0}^{\infty}\left[\left(\frac{n\pi}{l_x}\right)^2 A''_{\mathrm{II}n}(t)\sin\frac{n\pi}{l_x}x\int_0^z\int_{-h\mathrm{II}}^{\eta} B_{\mathrm{II}n}(\xi)\,d\xi d\eta\right], \tag{71}$$

$$\sum_{n=0}^{\infty} C''_{\mathrm{II}n}(t) D_{\mathrm{II}n}(z)\sin\frac{n\pi}{l_y}y$$
$$=-\frac{\partial p_{\mathrm{II}}|_{z=0}}{\rho_{\mathrm{II}}\partial y}+\sum_{n=0}^{\infty}\left[\left(\frac{n\pi}{l_y}\right)^2 C''_{\mathrm{II}n}(t)\sin\frac{n\pi}{l_y}y\int_0^z\int_{-h\mathrm{II}}^{\eta} D_{\mathrm{II}n}(\xi)\,d\xi d\eta\right]. \tag{72}$$

If Eqs. (71) and (72) are differentiated by z, equations of the same form as Eq. (67) are obtained as follows:

$$\left.\begin{aligned} B'_{\mathrm{II}n}(z)&=\left(\frac{n\pi}{l_x}\right)^2\int_{-h\mathrm{II}}^{z} B_{\mathrm{II}n}(z)\,dz,\\ D'_{\mathrm{II}n}(z)&=\left(\frac{n\pi}{l_y}\right)^2\int_{-h\mathrm{II}}^{z} D_{\mathrm{II}n}(z)\,dz.\end{aligned}\right\} \tag{73}$$

The solutions of Eq. (73) are given by

$$\left.\begin{aligned} B_{\mathrm{II}n}(z)&=\cosh\frac{n\pi}{l_x}(z+h_{\mathrm{II}}),\\ D_{\mathrm{II}n}(z)&=\cosh\frac{n\pi}{l_y}(z+h_{\mathrm{II}}).\end{aligned}\right\} \tag{74}$$

The substitution of Eq. (74) into Eqs. (71) and (72) yields the following equations of forced oscillations:

$$\sum_{n=0}^{\infty} A''_{\text{II}n}(t)\cosh\frac{n\pi}{l_x}h_{\text{II}}\sin\frac{n\pi}{l_x}x=-\frac{1}{\rho_{\text{II}}}\frac{\partial p_{\text{II}}|_{z=0}}{\partial x}-f''_H(t)\cos\alpha, \tag{75}$$

$$\sum_{n=0}^{\infty} C''_{\text{II}n}(t)\cosh\frac{n\pi}{l_y}h_{\text{II}}\sin\frac{n\pi}{l_y}y=-\frac{1}{\rho_{\text{II}}}\frac{\partial p_{\text{II}}|_{z=0}}{\partial y}-f''_H(t)\sin\alpha. \tag{76}$$

The substitution of Eq. (48) into Eqs. (75) and (76) gives

$$\left.\begin{aligned}&\rho_{\text{II}}\sum_{n=0}^{\infty} A''_{\text{II}n}(t)\cosh\frac{n\pi}{l_x}h_{\text{II}}\sin\frac{n\pi}{l_x}x\\&=-\frac{\partial p_{\text{I}}|_{z=0}}{\partial x}-(\rho_{\text{II}}-\rho_{\text{I}})(g+f''_V(t))\frac{\partial\zeta}{\partial x}-\rho_{\text{II}}f''_H(t)\cos\alpha,\\&\rho_{\text{II}}\sum_{n=0}^{\infty} C''_{\text{II}n}(t)\cosh\frac{n\pi}{l_y}h_{\text{II}}\sin\frac{n\pi}{l_y}y\\&=-\frac{\partial p_{\text{I}}|_{z=0}}{\partial y}-(\rho_{\text{II}}-\rho_{\text{I}})(g+f''_V(t))\frac{\partial\zeta}{\partial y}-\rho_{\text{II}}f''_H(t)\sin\alpha.\end{aligned}\right\} \tag{77}$$

Since $\frac{\partial p_{\text{I}}|_{z=0}}{\partial x}$ and $\frac{\partial p_{\text{I}}|_{z=0}}{\partial y}$ can be obtained from Eqs. (69) and (70), and ζ is given by Eq. (59), Eq. (77) can be rewritten, by using the relation in Eq. (60), as

$$\begin{aligned}&\sum_{n=0}^{\infty}\left\{1+\frac{\rho_{\text{I}}\tanh\frac{n\pi}{l_x}h_{\text{II}}}{\rho_{\text{II}}\tanh\frac{n\pi}{l_x}h_{\text{I}}}\right\}A''_{\text{II}n}(t)\cosh\frac{n\pi}{l_x}h_{\text{II}}\sin\frac{n\pi}{l_x}x\\&+\left(1-\frac{\rho_{\text{I}}}{\rho_{\text{II}}}\right)(g+f''_V(t))\sum_{n=0}^{\infty}\frac{n\pi}{l_x}A_{\text{II}n}(t)\sin\frac{n\pi}{l_x}x\sinh\frac{n\pi}{l_x}h_{\text{II}}\\&=-\left(1-\frac{\rho_{\text{I}}}{\rho_{\text{II}}}\right)f''_H(t)\cos\alpha,\end{aligned} \tag{78}$$

$$\begin{aligned}&\sum_{n=0}^{\infty}\left\{1+\frac{\rho_{\text{I}}\tanh\frac{n\pi}{l_y}h_{\text{II}}}{\rho_{\text{II}}\tanh\frac{n\pi}{l_y}h_{\text{I}}}\right\}C''_{\text{II}n}(t)\cosh\frac{n\pi}{l_y}h_{\text{II}}\sin\frac{n\pi}{l_y}y\\&+\left(1-\frac{\rho_{\text{I}}}{\rho_{\text{II}}}\right)(g+f''_V(t))\sum_{n=0}^{\infty}\frac{n\pi}{l_y}C_{\text{II}n}(t)\sinh\frac{n\pi}{l_y}h_{\text{II}}\sin\frac{n\pi}{l_y}y\\&=-\left(1-\frac{\rho_{\text{I}}}{\rho_{\text{II}}}\right)f''_H(t)\sin\alpha.\end{aligned} \tag{79}$$

By multiplying Eqs. (78) and (79) by $\sin(n\pi x/l_x)$ and $\sin(n\pi y/l_y)$ respectively and integrating them within their corresponding lengths of the tank, the summation symbol is eliminated, and thus

$$A''_{\text{II}n}(t)+\frac{\left(1-\frac{\rho_{\text{I}}}{\rho_{\text{II}}}\right)\frac{n\pi}{l_x}\tanh\frac{n\pi}{l_x}h_{\text{II}}}{\left\{1+\frac{\rho_{\text{I}}\tanh\frac{n\pi}{l_x}h_{\text{II}}}{\rho_{\text{II}}\tanh\frac{n\pi}{l_x}h_{\text{I}}}\right\}}\{g+f''_V(t)\}A_{\text{II}n}(t)$$

$$=-\left(1-\frac{\rho_{\mathrm{I}}}{\rho_{\mathrm{II}}}\right)\frac{2[1-(-1)^n]}{n\pi}f''_H(t)\cos\alpha\bigg/\left\{1+\frac{\rho_{\mathrm{I}}\tanh\frac{n\pi}{l_x}h_{\mathrm{II}}}{\rho_{\mathrm{II}}\tanh\frac{n\pi}{l_x}h_{\mathrm{I}}}\right\}\cosh\frac{n\pi}{l_x}h_{\mathrm{II}}, \tag{80}$$

$$C''_{\mathrm{II}n}(t)+\frac{\left(1-\frac{\rho_{\mathrm{I}}}{\rho_{\mathrm{II}}}\right)\frac{n\pi}{l_y}\tanh\frac{n\pi}{l_y}h_{\mathrm{II}}}{1+\left\{\frac{\rho_{\mathrm{I}}\tanh\frac{n\pi}{l_y}h_{\mathrm{II}}}{\rho_{\mathrm{II}}\tanh\frac{n\pi}{l_y}h_{\mathrm{I}}}\right\}}\{g+f''_V(t)\}C_{\mathrm{II}n}(t)$$

$$=-\left(1-\frac{\rho_{\mathrm{I}}}{\rho_{\mathrm{II}}}\right)\frac{2[1-(-1)^n]}{n\pi}f''_H(t)\sin\alpha\bigg/\left\{1+\frac{\rho_{\mathrm{I}}\tanh\frac{n\pi}{l_y}h_{\mathrm{II}}}{\rho_{\mathrm{II}}\tanh\frac{n\pi}{l_y}h_{\mathrm{I}}}\right\}\cosh\frac{n\pi}{l_y}h_{\mathrm{II}}. \tag{81}$$

The initial conditions of $A_{\mathrm{II}n}(t)$ and $C_{\mathrm{II}n}(t)$ which satisfy Eqs. (52) and (53) are expressed as

$$\left.\begin{array}{l}A'_{\mathrm{II}n}(t\leq 0)=0\ ,\ \ A_{\mathrm{II}n}(t\leq 0)=0,\\ C'_{\mathrm{II}n}(t\leq 0)=0\ ,\ \ C_{\mathrm{II}n}(t\leq 0)=0.\end{array}\right\} \tag{82}$$

If Eqs. (80) and (81) are solved for given functions of $f_H(t)$ and $f_V(t)$, the displacement of the boundary surface between the two liquids is easily obtained by substituting the solutions into Eq. (59).

$$\zeta=-\sum_{n=0}^{\infty}A_{\mathrm{II}n}(t)\cos\frac{n\pi}{l_x}x\sinh\frac{n\pi}{l_x}h_{\mathrm{II}}$$
$$-\sum_{n=0}^{\infty}C_{\mathrm{II}n}(t)\cos\frac{n\pi}{l_y}y\sinh\frac{n\pi}{l_y}h_{\mathrm{II}}. \tag{83}$$

The values of $p_{\mathrm{I}}|_{z=0}$ and $p_{\mathrm{II}}|_{z=0}$ are needed in order to obtain the formulas of the fluid pressures. The pressure $p_{\mathrm{I}}|_{z=0}$ is given by the combination of the integrated results of Eq. (69) with respect to x and Eq. (70) with respect to y as

$$p_{\mathrm{I}}|_{z=0}=\rho_{\mathrm{I}}\sum_{n=0}^{\infty}\left[\frac{l_x}{n\pi}A''_{\mathrm{I}n}(t)\left(\cos\frac{n\pi}{l_x}x-\cos\frac{n\pi}{2}\right)\cosh\frac{n\pi}{l_x}h_{\mathrm{I}}\right.$$
$$\left.+\frac{l_y}{n\pi}C''_{\mathrm{I}n}(t)\left(\cos\frac{n\pi}{l_y}x-\cos\frac{n\pi}{2}\right)\cosh\frac{n\pi}{l_y}h_{\mathrm{I}}\right]$$
$$-\rho_{\mathrm{I}}\left\{\left(x-\frac{l_x}{2}\right)\cos\alpha+\left(y-\frac{l_y}{2}\right)\sin\alpha\right\}f''_H(t)+[p_{\mathrm{I}}|_{z=0}]_{x=\frac{l_x}{2},y=\frac{l_y}{2}}, \tag{84}$$

where $[p_{\mathrm{I}}|_{z=0}]_{x=\frac{l_x}{2},y=\frac{l_y}{2}}$ is an intgral constant and may be a function of t only.

Combining Eqs. (75) and (76) gives

$$p_{\mathrm{II}}|_{z=0}=\rho_{\mathrm{II}}\sum_{n=0}^{\infty}\left[\frac{l_x}{n\pi}A''_{\mathrm{II}n}(t)\left(\cos\frac{n\pi}{l_x}x-\cos\frac{n\pi}{2}\right)\cosh\frac{n\pi}{l_x}h_{\mathrm{II}}\right.$$
$$\left.+\frac{l_y}{n\pi}C''_{\mathrm{II}n}(t)\left(\cos\frac{n\pi}{l_y}y-\cos\frac{n\pi}{2}\right)\cosh\frac{n\pi}{l_y}h_{\mathrm{II}}\right.$$
$$-\rho_{\mathrm{II}}\left\{\left(x-\frac{l_x}{2}\right)\cos\alpha+\left(y-\frac{l_y}{2}\right)\sin\alpha\right\}f''_H(t)+[p_{\mathrm{II}}|_{z=0}]_{x=\frac{l_x}{2},y=\frac{l_y}{2}}, \tag{85}$$

where $[p_{\mathrm{II}}|_{z=0}]_{x=\frac{l_x}{2},y=\frac{l_y}{2}}$ is also an integral constant.

Since Eq. (48) relates $p_{\mathrm{I}}|_{z=0}$ to $p_{\mathrm{II}}|_{z=0}$, the substitution of Eqs. (84) and (85) into Eq. (48) gives the following relation:

$$[p_{\mathrm{I}}|_{z=0}]_{x=\frac{l_x}{2},y=\frac{l_y}{2}}=[p_{\mathrm{II}}|_{z=0}]_{x=\frac{l_x}{2},y=\frac{l_y}{2}}. \tag{86}$$

Since at time $t=0$, there exists a static fluid pressure distribution of

$$[p_{\mathrm{I}}|_{z=0}]_{x=\frac{l_x}{2},y=\frac{l_y}{2}}=p_0+\rho_{\mathrm{I}}gh_{\mathrm{I}}, \tag{87}$$

where p_0 is a preliminary weighted pressure of the fluids, which may be a function t.

By the relation in Eq. (86) and substitution of Eq. (87) into Eqs. (84) and (85), the integral constants of $p_{\mathrm{I}}|_{z=0}$ and $p_{\mathrm{II}}|_{z=0}$ are determined. Finally, we can obtain the fluid pressures from Eqs. (61) and (62), thus:

$$\begin{aligned}p_{\mathrm{I}}=&p_0+\rho_{\mathrm{I}}g(h_{\mathrm{I}}-z)-\rho_{\mathrm{I}}f_V''(t)z\\&-\rho_{\mathrm{I}}\left\{\left(x-\frac{l_x}{2}\right)\cos\alpha+\left(y-\frac{l_y}{2}\right)\sin\alpha\right\}f_H''(t)\\&+\rho_{\mathrm{I}}\sum_{n=0}^{\infty}\left[\frac{l_x}{n\pi}A_{\mathrm{I}n}''(t)\left\{\cosh\frac{n\pi}{l_x}(z-h_{\mathrm{I}})\cos\frac{n\pi}{l_x}x-\cosh\frac{n\pi}{l_x}h_{\mathrm{I}}\cos\frac{n\pi}{2}\right\}\right.\\&\left.+\frac{l_y}{n\pi}C_{\mathrm{I}n}''(t)\left\{\cosh\frac{n\pi}{l_y}(z-h_{\mathrm{I}})\cos\frac{n\pi}{l_y}y-\cosh\frac{n\pi}{l_y}h_{\mathrm{I}}\cos\frac{n\pi}{2}\right\}\right],\end{aligned} \tag{88}$$

$$\begin{aligned}p_{\mathrm{II}}=&p_0+g(\rho_{\mathrm{I}}h_{\mathrm{I}}-\rho_{\mathrm{II}}z)-\rho_{\mathrm{II}}f_V''(z)\\&-\rho_{\mathrm{II}}\left\{\left(x-\frac{l_x}{2}\right)\cos\alpha+\left(y-\frac{l_y}{2}\right)\sin\alpha\right\}f_H''(t)\\&+\rho_{\mathrm{II}}\sum_{n=0}^{\infty}\left[\frac{l_x}{n\pi}A_{\mathrm{II}n}''(t)\left\{\cosh\frac{n\pi}{l_x}(z+h_{\mathrm{II}})\cos\frac{n\pi}{l_x}x-\cosh\frac{n\pi}{l_x}h_{\mathrm{II}}\cos\frac{n\pi}{2}\right\}\right.\\&\left.+\frac{l_y}{n\pi}C_{\mathrm{II}n}''(t)\left\{\cosh\frac{n\pi}{l_y}(z+h_{\mathrm{II}})\cos\frac{n\pi}{l_y}y-\cosh\frac{n\pi}{l_y}h_{\mathrm{II}}\cos\frac{n\pi}{2}\right\}\right].\end{aligned} \tag{89}$$

If we take p_0 and ρ_{I} as zero, these equations are applicable to the corresponding problems encountered inside a rectangular ground storage tank.

5.2 Circular Tanks

When the dynamic equations of Eqs. (43) and (44) and the equation of continuity of fluid mass of Eqs. (45) and (46) are transformed into the cylindrical coordinates (r, θ, z), under the condition that the horizontal tank displacement occurs along the line of $\theta=0$, they are expressed as follows:

$$\left.\begin{aligned}\frac{\partial u_{r\mathrm{I}}}{\partial t}&=-\frac{1}{\rho_{\mathrm{I}}}\frac{\partial p_{\mathrm{I}}}{\partial r}-f_H''(t)\cos\theta,\\\frac{\partial u_{\theta\mathrm{I}}}{\partial t}&=-\frac{1}{\rho_{\mathrm{I}}}\frac{\partial p_{\mathrm{I}}}{r\partial\theta}-f_H''(t)\sin\theta,\\\frac{\partial w_{\mathrm{I}}}{\partial t}&=-\frac{1}{\rho_{\mathrm{I}}}\frac{\partial p_{\mathrm{I}}}{\partial z}-g-f_V''(t),\end{aligned}\right\} \tag{90}$$

$$\left.\begin{aligned}\frac{\partial u_{r\mathrm{II}}}{\partial t}&=-\frac{1}{\rho_{\mathrm{II}}}\frac{\partial p_{\mathrm{II}}}{\partial r}-f_H''(t)\cos\theta,\\\frac{\partial u_{\theta\mathrm{II}}}{\partial t}&=-\frac{1}{\rho_{\mathrm{II}}}\frac{\partial p_{\mathrm{II}}}{r\partial\theta}-f_H''(t)\sin\theta,\\\frac{\partial w_{\mathrm{I}}}{\partial t}&=-\frac{1}{\rho_{\mathrm{II}}}\frac{\partial p_{\mathrm{II}}}{\partial z}-g-f_V''(t),\end{aligned}\right\} \tag{91}$$

$$\frac{\partial u_{r\mathrm{I}}}{\partial r}+\frac{u_{r\mathrm{I}}}{r}+\frac{\partial u_{\theta\mathrm{I}}}{r\partial\theta}+\frac{\partial w_{\mathrm{I}}}{\partial z}=0, \tag{92}$$

$$\frac{\partial u_{r\mathrm{II}}}{\partial r}+\frac{u_{r\mathrm{II}}}{r}+\frac{\partial u_{\theta\mathrm{I}}}{r\partial\theta}+\frac{\partial w_{\mathrm{II}}}{\partial z}=0, \tag{93}$$

where u_r, u_θ and w are the velocities of a fluid particle in the directions of r, θ and z, respectively. A schematic circular tank is shown in **Fig. 4**.

The conditions on the boundary surface between the two liquids are given by the same equations as Eqs. (47) and (48):

$$\frac{\partial\zeta}{\partial t}=w_{\mathrm{I}}|_{z=0}=w_{\mathrm{II}}|_{z=0}, \tag{94}$$

$$p_{\mathrm{II}}|_{z=0}=p_{\mathrm{I}}|_{z=0}+(\rho_{\mathrm{II}}-\rho_{\mathrm{I}})\{g+f_V''(t)\}\zeta. \tag{95}$$

The boundary conditions on the rigid wall of the circular tank are represented as follows:

$$u_{r\mathrm{I}}|_{r=r_0}=0\ ,\ \ u_{r\mathrm{II}}|_{r=r_0}=0, \tag{96}$$

$$w_{\mathrm{I}}|_{z=h\mathrm{I}}=0\ ,\ \ w_{\mathrm{II}}|_{z=-h\mathrm{II}}=0, \tag{97}$$

where r_0 is the inner radius of the tank, and h_{I} and h_{II} are the thicknesses of the upper and the lower layers, respectively, as shown in **Fig. 4**.

The initial conditions are given in the same form as Eq. (52):

$$\left.\begin{array}{ll} u_{r\mathrm{I}}|_{t\le 0}=0\ , & u_{r\mathrm{II}}|_{t\le 0}=0,\\ u_{\theta\mathrm{I}}|_{t\le 0}=0\ , & u_{\theta\mathrm{II}}|_{t\le 0}=0,\\ w_{\mathrm{I}}|_{t\le 0}=0\ , & w_{\mathrm{II}}|_{t\le 0}=0. \end{array}\right\} \tag{98}$$

The displacement $(X_r,\ X_\theta,\ Z)$ of a fluid particle in the r, θ and z directions is given in the same form as Eq. (53):

$$\left.\begin{array}{ll} X_{r\mathrm{I}}=\int_0^t u_{r\mathrm{I}}dt, & X_{r\mathrm{II}}=\int_0^t u_{r\mathrm{II}}dt,\\ X_{\theta\mathrm{I}}=\int_0^t u_{\theta\mathrm{I}}dt, & X_{\theta\mathrm{II}}=\int_0^t u_{\theta\mathrm{II}}dt,\\ Z_{\mathrm{I}}=\int_0^t w_{\mathrm{I}}dt, & Z_{\mathrm{II}}=\int_0^t w_{\mathrm{II}}dt. \end{array}\right\} \tag{99}$$

The forms of $u_{r\mathrm{I}}$ and $u_{r\mathrm{II}}$ which satisfy the boundary conditions of Eq. (96) are expressed as follows:

$$\left.\begin{array}{l} u_{r\mathrm{I}}=\sum\limits_{n,i}G'_{\mathrm{I}ni}(t)\,H_{\mathrm{I}ni}(z)\,J'_n(k_{ni}r)\cos n\theta,\\ u_{r\mathrm{II}}=\sum\limits_{n,i}G'_{\mathrm{II}ni}(t)\,H_{\mathrm{II}ni}(z)\,J'_n(k_{ni}r)\cos n\theta, \end{array}\right\} \tag{100}$$

where k_{ni} is the i-th solution of $J'_n(k_{ni}r_0)=0$ and $J_n(k_{ni}r)$ is a Bessel function of the first kind, which astisfies the following equation:

$$J''_n(k_{ni}r)+\frac{1}{k_{ni}r}J'_n(k_{ni}r)+\left\{1-\frac{n^2}{(k_{ni}r)^2}\right\}J_n(k_{ni}r)=0. \tag{101}$$

The first equations of Eqs. (90) and (91) are integrated with respect to r, yielding

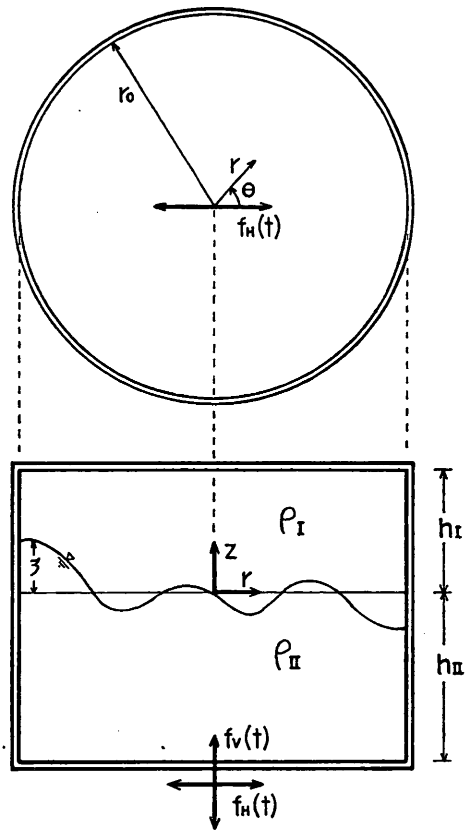

Fig. 4 Circular Tank

$$\left.\begin{aligned} p_{\mathrm{I}} &= p_{\mathrm{I}}|_{r=0} - \rho_{\mathrm{I}}\int_0^r \frac{\partial u_{r\mathrm{I}}}{\partial t}dr - rf''_H(t)\cos\theta, \\ p_{\mathrm{II}} &= p_{\mathrm{II}}|_{r=0} - \rho_{\mathrm{II}}\int_0^r \frac{\partial u_{r\mathrm{II}}}{\partial t}dr - rf''_H(t)\cos\theta, \end{aligned}\right\} \qquad (102)$$

and then the substitution of p_{I} and p_{II} of Eq. (102) into the second equations of Eqs. (90) and (91) gives

$$\left.\begin{aligned} \frac{\partial u_{\theta\mathrm{I}}}{\partial t} &= -\frac{1}{\rho_{\mathrm{I}}}\frac{\partial p_{\mathrm{I}}|_{r=0}}{r\partial\theta} + \frac{\partial}{r\partial\theta}\int_0^r \frac{\partial u_{r\mathrm{I}}}{\partial t}dr, \\ \frac{\partial u_{\theta\mathrm{II}}}{\partial t} &= -\frac{1}{\rho_{\mathrm{II}}}\frac{\partial p_{\mathrm{II}}|_{r=0}}{r\partial\theta} + \frac{\partial}{r\partial\theta}\int_0^r \frac{\partial u_{r\mathrm{I}}}{\partial t}dr. \end{aligned}\right\} \qquad (103)$$

When r approaches zero in Eq. (103), we get the following expressions:

$$\left.\begin{aligned} \lim_{r\to 0}\frac{\partial u_{\theta\mathrm{I}}}{\partial t} &= \lim_{r\to 0}\left\{-\frac{1}{\rho_{\mathrm{I}}}\frac{\partial p_{\mathrm{I}}|_{r=0}}{r\partial\theta}\right\} + \left.\frac{\partial^2 u_{r\mathrm{I}}}{\partial\theta\partial t}\right|_{r=0}, \\ \lim_{r\to 0}\frac{\partial u_{\theta\mathrm{II}}}{\partial t} &= \lim_{r\to 0}\left\{-\frac{1}{\rho_{\mathrm{II}}}\frac{\partial p_{\mathrm{II}}|_{r=0}}{r\partial\theta}\right\} + \left.\frac{\partial^2 u_{r\mathrm{II}}}{\partial\theta\partial t}\right|_{r=0}. \end{aligned}\right\} \qquad (104)$$

Since both $\partial u_{\theta\mathrm{I}}/\partial t$ and $\partial u_{\theta\mathrm{II}}/\partial t$ have finite values at the center of the tank, each first term of the right hand sides of Eq. (104) must vanish. Then, Eq. (103) is rewritten as

$$\left.\begin{aligned}\frac{\partial u_{\theta\mathrm{I}}}{\partial t}&=\frac{1}{r}\int_0^r\frac{\partial^2 u_{r\mathrm{I}}}{\partial\theta\partial t}dr,\\ \frac{\partial u_{\theta\mathrm{II}}}{\partial t}&=\frac{1}{r}\int_0^r\frac{\partial^2 u_{r\mathrm{II}}}{\partial\theta\partial t}dr.\end{aligned}\right\}\tag{105}$$

Substituting Eq. (100) into Eq. (105) and then integrating Eq. (105) with respect to t under the initial conditions of Eq. (98), we have

$$\left.\begin{aligned}u_{\theta\mathrm{I}}&=-\sum_{n,i}\frac{n}{k_{ni}r}G'_{\mathrm{I}ni}(t)H_{\mathrm{I}ni}(z)J_n(k_{ni}r),\\ u_{\theta\mathrm{II}}&=-\sum_{n,i}\frac{n}{k_{ni}r}G'_{\mathrm{II}ni}(t)H_{\mathrm{II}ni}(z)J_n(k_{ni}r).\end{aligned}\right\}\tag{106}$$

The substitution of Eqs. (100) and (106) into Eqs. (92) and (93) and their integration with respect to z under the boundary conditions of Eq. (97), give the following equations for w_{I} and w_{II}:

$$\left.\begin{aligned}w_{\mathrm{I}}&=\sum_{n,i}k_{ni}G'_{\mathrm{I}ni}(t)J_n(k_{ni}r)\cos n\theta\int_{h\mathrm{I}}^{z}H_{\mathrm{I}ni}(z)\,dz,\\ w_{\mathrm{II}}&=\sum_{n,i}k_{ni}G'_{\mathrm{II}ni}(t)J_n(k_{ni}r)\cos n\theta\int_{-h\mathrm{II}}^{z}H_{\mathrm{II}ni}(z)dz.\end{aligned}\right\}\tag{107}$$

By combining Eqs. (94) and (107), the following relation between $G_{\mathrm{I}ni}(t)$ and $G_{\mathrm{II}ni}(t)$ is derived:

$$G_{\mathrm{I}ni}(t)=G_{\mathrm{II}ni}(t)\int_{-h\mathrm{II}}^{0}H_{\mathrm{II}ni}(z)\,dz\Big/\int_{h\mathrm{I}}^{0}H_{\mathrm{I}ni}(z)\,dz.\tag{108}$$

Furthermore, the boundary surface displacement of ζ is given by substituting Eq. (107) into Eq. (94):

$$\zeta=\sum_{n,i}k_{ni}G_{\mathrm{II}ni}(t)\,J_n(k_{ni}r)\cos n\theta\int_{-h\mathrm{II}}^{0}H_{\mathrm{II}ni}(z)\,dz.\tag{109}$$

From the substitution of Eq. (107) into the third equations of Eqs. (90) and (91), and their integration with respect to z, the following fluid pressures of p_{I} and p_{II} are obtained:

$$\begin{aligned}p_{\mathrm{I}}=&\,p_{\mathrm{I}}|_{z=0}-\rho_{\mathrm{I}}\sum_{n,i}k_{ni}G''_{\mathrm{I}ni}(t)\,J_n(k_{ni}r)\cos n\theta\int_0^z\int_{h\mathrm{I}}^{\eta}H_{\mathrm{I}ni}(\xi)d\xi d\eta\\ &-\rho_{\mathrm{I}}\{g+f''_V(t)\}z,\end{aligned}\tag{110}$$

$$\begin{aligned}p_{\mathrm{II}}=&\,p_{\mathrm{II}}|_{z=0}-\rho_{\mathrm{II}}\sum_{n,i}k_{ni}G''_{\mathrm{II}ni}(t)\,J_n(k_{ni}r)\cos n\theta\int_0^z\int_{-h\mathrm{II}}^{\eta}H_{\mathrm{II}ni}(\xi)d\xi d\eta\\ &-\rho_{\mathrm{II}}\{g+f''_V(t)\}z.\end{aligned}\tag{111}$$

The substitution of p_{I} of Eq. (110) and $u_{r\mathrm{I}}$ of the first equation of Eq. (100) into the first equation of Eq. (90) gives

$$\begin{aligned}&\sum_{n,i}G''_{\mathrm{I}ni}(t)H_{\mathrm{I}ni}(z)\,J'_n(k_{ni}r)\cos n\theta\\ &=-\frac{1}{\rho_{\mathrm{I}}}\frac{\partial p_{\mathrm{I}}|_{z=0}}{\partial r}+\sum_{n,i}k_{ni}^2G''_{\mathrm{I}ni}(t)\,J''_n(k_{ni}r)\cos n\theta\int_0^z\int_{h\mathrm{I}}^{\eta}H_{\mathrm{I}ni}(\xi)d\xi d\eta\\ &\quad-f''_H(t)\cos\theta.\end{aligned}\tag{112}$$

The differentiation of Eq. (112) by z gives the following equation with respect to $H_{\mathrm{I}ni}(z)$:

$$H'_{\mathrm{I}ni}(z)=k_{ni}^2\int_{h\mathrm{I}}^{z}H_{\mathrm{I}ni}(z)\,dz.\tag{113}$$

The solution of Eq. (113) can be easily obtained as

$$H_{\mathrm{I}ni}(z)=\cosh k_{ni}(z-h_{\mathrm{I}}). \tag{114}$$

By using Eq. (114), Eq. (112) can be rewritten as

$$\sum_{n,i} G''_{\mathrm{I}ni}(t)\cosh k_{ni}h_{\mathrm{I}}\; J'_n(k_{ni}r)\cos n\theta$$
$$=-\frac{1}{\rho_{\mathrm{I}}}\frac{\partial p_{\mathrm{I}}|_{z=0}}{\partial r}-f''_H(t)\cos\theta. \tag{115}$$

Similarly to $H_{\mathrm{I}ni}(z)$, $H_{\mathrm{II}ni}(z)$ is derived as

$$H_{\mathrm{II}ni}(z)=\cosh k_{ni}(z+h_{\mathrm{II}}). \tag{116}$$

Consequently, the following equation is obtained:

$$\sum_{n,i} G''_{\mathrm{II}ni}(t)\cosh k_{ni}h_{\mathrm{II}}\; J'_n(k_{ni}r)\cos n\theta$$
$$=-\frac{1}{\rho_{\mathrm{II}}}\frac{\partial p_{\mathrm{II}}|_{z=0}}{\partial r}-f''_H(t)\cos\theta. \tag{117}$$

By using the relation between $p_{\mathrm{I}}|_{z=0}$ and $p_{\mathrm{II}}|_{z=0}$ in Eq. (95), Eq. (117) can be rewritten as

$$\sum_{n,i} G''_{\mathrm{II}ni}(t)\cosh k_{ni}h_{\mathrm{II}}\; J'_n(k_{ni}r)\cos n\theta$$
$$=-\frac{1}{\rho_{\mathrm{II}}}\frac{\partial p_{\mathrm{I}}|_{z=0}}{\partial r}-\left(1-\frac{\rho_{\mathrm{I}}}{\rho_{\mathrm{II}}}\right)\left\{g+f''_V(t)\right\}\frac{\partial\zeta}{\partial r}-f''_H(t)\cos\theta. \tag{118}$$

Since ζ has already been obtained in Eq. (109), the combination of Eqs. (115) and (118) gives

$$\sum_{n,i} G''_{\mathrm{II}ni}(t)\, J'_n(k_{ni}r)\cosh k_{ni}h_{\mathrm{II}}\cos n\theta$$
$$=\frac{\rho_{\mathrm{I}}}{\rho_{\mathrm{II}}}\sum_{n,i} G''_{\mathrm{I}ni}(t)\, J'_n(k_{ni}r)\cosh k_{ni}h_{\mathrm{I}}\cos n\theta$$
$$-\left(1-\frac{\rho_{\mathrm{I}}}{\rho_{\mathrm{II}}}\right)\{g+f''_V(t)\}\sum_{n,i} k_{ni}G_{\mathrm{II}ni}(t)\, J'_n(k_{ni}r)\sinh k_{ni}h_{\mathrm{II}}\cos n\theta$$
$$-\left(1-\frac{\rho_{\mathrm{I}}}{\rho_{\mathrm{II}}}\right)f''_H(t)\cos\theta. \tag{119}$$

The relation between $G_{\mathrm{I}ni}(t)$ and $G_{\mathrm{II}ni}(t)$ found in Eq. (108), can now be rewritten, by using Eqs. (114) and (116), as

$$G_{\mathrm{I}ni}(t)=-G_{\mathrm{II}ni}(t)\sinh k_{ni}h_{\mathrm{II}}/\sinh k_{ni}h_{\mathrm{I}}. \tag{120}$$

The substitution of Eq. (120) into Eq. (119) gives

$$\sum_{n,i}\left\{1+\frac{\rho_{\mathrm{I}}\tanh k_{ni}h_{\mathrm{II}}}{\rho_{\mathrm{II}}\tanh k_{ni}h_{\mathrm{I}}}\right\}G''_{\mathrm{II}ni}(t)\, J'_n(k_{ni}r)\cosh k_{ni}h_{\mathrm{II}}\cos n\theta$$
$$+\left(1-\frac{\rho_{\mathrm{I}}}{\rho_{\mathrm{II}}}\right)\{g+f''_V(t)\}\sum_{n,i} k_{ni}G_{\mathrm{II}ni}(t)\, J'_n(k_{ni}r)\sinh k_{ni}h_{\mathrm{II}}\cos n\theta$$
$$=-\left(1-\frac{\rho_{\mathrm{I}}}{\rho_{\mathrm{II}}}\right)f''_H(t)\cos\theta. \tag{121}$$

By multiplying Eq. (121) by $\cos n\theta$ and integrating it with respect to θ from 0 to 2π, we have the following equations:

if $n=1$:

$$\sum_i \left\{1+\frac{\rho_{\mathrm{I}} \tanh k_{1i}h_{\mathrm{II}}}{\rho_{\mathrm{II}} \tanh k_{1i}h_{\mathrm{I}}}\right\} G''_{\mathrm{II}1i}(t)\, J'_1(k_{1i}r) \cosh k_{1i}h_{\mathrm{II}}$$

$$+\left(1-\frac{\rho_{\mathrm{I}}}{\rho_{\mathrm{II}}}\right)\{g+f''_V(t)\}\sum_i k_{1i}G_{\mathrm{II}1i}(t)\, J'_1(k_{1i}r) \sinh k_{1i} h_{\mathrm{II}}$$

$$=-\left(1-\frac{\rho_{\mathrm{I}}}{\rho_{\mathrm{II}}}\right)f''_H(t). \tag{122}$$

if $n \neq 1$:

$$\sum_i \left\{1+\frac{\rho_{\mathrm{I}} \tanh k_{ni}h_{\mathrm{II}}}{\rho_{\mathrm{II}} \tanh k_{ni}h_{\mathrm{I}}}\right\} G''_{\mathrm{II}ni}(t)\, J'_n(k_{ni}r) \cosh k_{ni}h_{\mathrm{II}}$$

$$+\left(1-\frac{\rho_{\mathrm{I}}}{\rho_{\mathrm{II}}}\right)\{g+f''_V(t)\}\sum_i k_{ni}G_{\mathrm{II}ni}(t)\, J'_n(k_{ni}r) \sinh k_{ni} h_{\mathrm{II}}$$

$$=0. \tag{123}$$

In the case of $n \neq 1$, Eq. (123) is rewritten as follows:

$$\left\{1+\frac{\rho_{\mathrm{I}} \tanh k_{ni}h_{\mathrm{II}}}{\rho_{\mathrm{II}} \tanh k_{ni}h_{\mathrm{I}}}\right\} G''_{\mathrm{II}ni}(t)+\left(1-\frac{\rho_{\mathrm{I}}}{\rho_{\mathrm{II}}}\right)\{g+f''_V(t)\}k_{ni}G_{\mathrm{II}ni}(t) \tanh k_{ni}h_{\mathrm{II}}$$

$$=0. \tag{124}$$

If $f_V(t)$ vanishes in Eq. (124) and the boundary surface has some initial displacement from the still surface, then Eq. (124) becomes an equation for free oscillations. However, it has a solution of $G_{\mathrm{II}ni}(t)=0$ under the initial conditions given by Eqs. (98) and (99). Therefore, only Eq. (122) is significant.

By integrating Eq. (122) with respect to r, multiplying both sides by $rJ_1(k_{1i}r)$, and integrating again with respect to r from 0 to r_0, the following equation is derived:

$$\left\{1+\frac{\rho_{\mathrm{I}} \tanh k_{1i}h_{\mathrm{II}}}{\rho_{\mathrm{II}} \tanh k_{1i}h_{\mathrm{I}}}\right\} G''_{\mathrm{II}1i}(t)$$

$$+\left(1-\frac{\rho_{\mathrm{I}}}{\rho_{\mathrm{II}}}\right)\{g+f''_V(t)\}\, k_{1i}G_{\mathrm{II}1i}(t) \tanh k_{1i}h_{\mathrm{II}}$$

$$=-\left(1-\frac{\rho_{\mathrm{I}}}{\rho_{\mathrm{II}}}\right)f''_H(t)\frac{I_i}{\cosh k_{1i}h_{\mathrm{II}}}, \tag{125}$$

$$\text{where } I_i=\frac{2k_{1i}r_0}{\{(k_{1i}r_0)^2-1\}J_1(k_{1i}r_0)}. \tag{126}$$

If we solve Eq. (125) for the initial conditions, the boundary surface displacement of ζ and the fluid pressures of p_{I} and p_{II} can be obtained.

The boundary surface displacement is given by

$$\zeta=\sum_i G_{\mathrm{II}1i}(t)J_1(k_{1i}r) \sinh k_{1i}h_{\mathrm{II}} \cos\theta. \tag{127}$$

The fluid pressures can be derived in the same way as for the case of a rectangular tank. First we get $p_{\mathrm{I}}|_{z=0}$ and $p_{\mathrm{II}}|_{z=0}$ by the integration of Eqs. (115) and (117). We obtain

$$\left.\begin{aligned}
p_{\mathrm{I}}|_{z=0}=&-\rho_{\mathrm{I}}\sum_i\frac{1}{k_{1i}}G''_{\mathrm{II}1i}(t) \cosh k_{1i}h_{\mathrm{I}}\, J_1(k_{1i}r) \cos\theta\\
&-\rho_{\mathrm{I}} r f''_H(t) \cos\theta+p_{\mathrm{I}}|_{z=0,\, r=0},\\
\text{and}&\\
p_{\mathrm{II}}|_{z=0}=&-\rho_{\mathrm{II}}\sum_i\frac{1}{k_{1i}}G''_{\mathrm{II}1i}(t) \cosh k_{1i}h_{\mathrm{II}}\, J_1(k_{1i}r) \cos\theta\\
&-\rho_{\mathrm{II}} r f''_H(t) \cos\theta+p_{\mathrm{II}}|_{z=0,\, r=0},
\end{aligned}\right\} \tag{128}$$

where $p_{\mathrm{I}}|_{z=0,\ r=0}$ and $p_{\mathrm{II}}|_{z=0,\ r=0}$ are integral constants.

The relation between $p_{\mathrm{I}}|_{z=0}$ and $p_{\mathrm{II}}|_{z=0}$ given in Eq. (95) gives

$$p_{\mathrm{I}}|_{z=0,\ r=0}=p_{\mathrm{II}}|_{z=0,\ r=0}. \tag{129}$$

Since the pressures show an initial static pressure distributions at $t=0$, then:

$$p_{\mathrm{I}}|_{z=0,\ r=0}=p_0+\rho_{\mathrm{I}}gh_{\mathrm{I}}, \tag{130}$$

where p_0 is a preliminary weighted pressure, which may be a function of time.

Consequently, the fluid pressures in each layer are given by the following equations:

$$p_{\mathrm{I}}=p_0+\rho_{\mathrm{I}}g(h_{\mathrm{I}}-z)-\rho_{\mathrm{I}}\{f_V''(t)z+rf_H''(t)\cos\theta\}$$
$$-\rho_{\mathrm{I}}\sum_i\frac{1}{k_{1i}}G_{\mathrm{I}1i}''(t)\,J_1(k_{1i}r)\cosh k_{1i}(z-h_{\mathrm{I}})\cos\theta \tag{131}$$

$$p_{\mathrm{II}}=p_0+g(\rho_{\mathrm{I}}h_{\mathrm{I}}-\rho_{\mathrm{II}}z)-\rho_{\mathrm{II}}\{f_V''(t)z+rf_H''(t)\cos\theta\}$$
$$-\rho_{\mathrm{II}}\sum_i\frac{1}{k_{1i}}G_{\mathrm{II}1i}''(t)\,J_1(k_{1i}r)\cosh k_{1i}(z+h_{\mathrm{II}})\cos\theta \tag{132}$$

As shown in the case of a rectangular tank, the above equations are applicable to the corresponding problems inside a circular ground storage tank.

6. Solution of Basic Differential Equations

The differential equations in Eqs. (80), (81) and (125), derived in the previous chapter, have to be solved under proper initial conditions in order to compute the displacement of the boundary surface between the liquids and the dynamic fluid pressures exerted upon the walls of the tank. Since the differential equations show the same form, they can be expressed by the following representative form:

$$q''(t)+\alpha_n\{g+f_V''(t)\}q(t)=-\beta_nf_H''(t), \tag{133}$$

where $q(t)$ represents $A_{\mathrm{II}n}(t)$, $C_{\mathrm{II}n}(t)$ or $G_{\mathrm{II}1i}(t)$, $f_H(t)$ and $f_V(t)$ represent the horizontal and the vertical tank movements, respectively, and α_n, β_n and g are constants.

It is very complex to derive the analitical solutions of Eq. (133), which includes a function of t as a coefficient of $q(t)$. Therefore, it is convenient to consider two cases: one is the case of $f_V(t)\equiv 0$, and the other is the case where $f_V(t)$ has some nonzero values which depend on time.

6.1 The Case of $f_V(t)\equiv 0$

In this case, Eq. (133) becomes a linear differential equation with constant coefficients:

$$q''(t)+\alpha_ngq(t)=-\beta_nf_H''(t). \tag{134}$$

The initial conditions of $q(t)$ and $f_H(t)$ are given as follows:

$$\left.\begin{array}{ll} q'(t)=0, & q(t)=0, \\ f_H'(t)=0, & f_H(t)=0, \quad \text{for } t\leq 0. \end{array}\right\} \tag{135}$$

If the Laplace transformation, which is generally effective for an initial value problem, is applied to Eq. (134), then it is reduced to

$$q^*(s)=-\frac{\beta_ns^2}{s^2+\alpha_ng}f_H^*(s), \tag{136}$$

where s is a parameter of the Laplace transformation, and $q^*(s)$ and $f_H^*(s)$ represent the following transforms of $q(t)$ and $f_H(t)$, respectively:

$$\left.\begin{aligned} q^*(s) &= \int_0^\infty q(t)e^{-st}dt, \\ f_H^*(s) &= \int_0^\infty f_H(t)e^{-st}dt. \end{aligned}\right\} \tag{137}$$

Since the inverse transform of $q^*(s)$ gives $q(t)$, $q(t)$ is obtained by the residue method as

$$q(t) = -\beta_n f_H(t) + \beta_n \omega \int_0^t \sin \omega(t-\tau) f_H(\tau) d\tau \tag{138}$$

where $\omega = \sqrt{\alpha_n g}$, which indicates a natural angular frequency of the fluid oscillation.

By using Eq. (138), $q(t)$ can be computed for any arbitrary horizontal tank movement. For instance, in the case of $f_H(t) = b_H \sin \Omega t$, $q(t)$ is expressed, by integrating the integral term in Eq. (138), as

$$q(t) = -\beta_n b_H \frac{\omega^2 - \Omega^2}{\Omega \omega} \left\{ \sin \omega t - \frac{\Omega}{\omega} \sin \Omega t \right\} \quad \text{for } \omega \neq \Omega, \tag{139}$$

$$q(t) = -\frac{\beta_n}{2} b_H \{ \sin \omega t + \omega t \cos \omega t \} \quad \text{for } \omega = \Omega. \tag{140}$$

Equation (139) indicates the case of non-resonance and Eq. (140) the case of resonance. In the latter case, the amplitude of $q(t)$ increases propotionally with time.

The resonance of lower natural frequencies is generally more influential for the problem of oscillations with multiple natural frequencies. We investigated this phenomenon.

We deal with a boundary surface displacement ζ inside a rectangular tank. In order to simplify the problem, we assume that the direction of the earthquake's action is parallel to the x-axis, that is, $C_{\mathrm{II}n}(t) = 0$, in Eq. (83). If the value of n is sufficiently large, $\tanh(n\pi h_{\mathrm{I}}/l_x) \approx 1$ and $\tanh(n\pi h_{\mathrm{II}}/l_x) \approx 1$ in Eq. (80). Therefore, α_n in Eq. (134) is proportional to n, while β_n is inversely proportional to n. Consequently, the natural frequency of ω is proportional to the root of n. Since the amplitude of ζ in Eq. (83) is approximately proportional to $t\omega\beta_n$, referring to Eq. (140), it becomes inversely proportional to the root of n as follows:

$$\zeta_{\mathrm{amp}} \propto \frac{t}{\sqrt{n}}, \tag{141}$$

where ζ_{amp} represents the amplitude of ζ.

Equation (141) implies that it takes about $\sqrt{n}$ times longer for ζ_{amp} of the n-th mode to reach the same height as that of the first mode. In consequence, resonant phenomena in higher modes are less critical problem than those in lower modes. Furthermore, if we take into account the damping of internal waves, the resonance in high modes becomes less important, because the energy dissipation of the waves becomes larger as the resonant modes become higher.

6.2 The Case of $f_V(t)$ having non-zero values

Since Eq. (133) includes a combination term $f_V(t)q(t)$, its analitical solution is very difficult and complex to obtain. We investigate the characteristic properties of the solution such as resonance conditions and a variation of angular frequencies, by obtaining approximate solutions excluding close resonance frequencies[18].

The functions of $f_V''(t)$ and $f_H''(t)$ are assumed to follow simple sinusoidal curves, which are given by

$$\left.\begin{aligned} f_V''(t) &= -a_V\gamma^2 \sin \gamma t, \\ f_H''(t) &= -b_H\Omega^2 \sin \Omega t, \end{aligned}\right\} \tag{142}$$

where a_V and b_H are the amplitudes of the tank displacement, and γ and Ω represent the angular frequencies of the tank movements.

The equation is rewritten as

$$q''(t)+\omega^2\{1-\varepsilon \sin \gamma t\}q(t)=E \sin \Omega t, \tag{143}$$

where $\omega=\sqrt{\alpha_n g}$, $\varepsilon=\dfrac{a_V\gamma^2}{g}$ and $E=\beta_n b_H \Omega^2$.

It is assumed that $q(t)$ does not show any resonance and that ε is a small quantity compared with unity, that is, $\varepsilon<1$. Then $q(t)$ is transformed to

$$q(t)=S(t)+U \sin \Omega t. \tag{144}$$

The substitution of Eq. (144) into Eq. (143) gives

$$S''(t)+\omega^2 S(t)=\varepsilon\omega^2\{S(t)+U \sin \Omega t\} \sin \Omega t, \tag{145}$$

where $U=E/(\omega^2-\Omega^2)$ and $\omega \fallingdotseq \Omega$.

If $\varepsilon=0$, the solution can be expressed as

$$S(t)=\eta_0 \sin \phi, \tag{146}$$

where $\phi=\omega t+\xi_0$, and the amplitude η_0 and the phase difference ξ_0 can be determined by the initial condition.

A small disturbance of ε sin γt may vary the values of η_0 and ϕ. So the quantities of $S(t)$, η_0 and ϕ are assumed to be expressed by the power series of ε as follows:

$$\left.\begin{aligned} S(t) &= \eta_0 \sin \phi+\varepsilon u_1(\eta_0, \phi, \sigma, \tau)+\varepsilon^2 u_2(\eta_0, \phi, \sigma, \tau)+\cdots\cdots, \\ \frac{d\eta_0}{dt} &= \varepsilon A_1(\eta_0)+\varepsilon^2 A_2(\eta_0)+\cdots\cdots, \\ \frac{d\phi}{dt} &= \omega+\varepsilon B_1(\eta_0)+\varepsilon^2 B_2(\eta_0)+\cdots\cdots, \end{aligned}\right\} \tag{147}$$

where $\sigma=\gamma t$, $\tau=\Omega t$, and u_1 and u_2 are presumed not to include the fundamental mode, that is,

$$\left.\begin{aligned} &\int_0^{2\pi} u_1(\eta_0, \phi, \sigma, \tau) \cos \phi d\phi=0, \\ &\int_0^{2\pi} u_2(\eta_0, \phi, \sigma, \tau) \cos \phi d\phi=0, \\ &\cdots\cdots\cdots\cdots\cdots\cdots\cdots\cdots \\ \text{and}\quad &\int_0^{2\pi} u_1(\eta_0, \phi, \sigma, \tau) \sin \phi d\phi=0, \\ &\int_0^{2\pi} u_2(\eta_0, \phi, \sigma, \tau) \sin \phi d\phi=0, \\ &\cdots\cdots\cdots\cdots\cdots\cdots\cdots\cdots \end{aligned}\right\} \tag{148}$$

If we substitute Eq. (147) into Eq. (145) and equate the coefficients of ε's of the same power in the right and the left hand sides of Eq. (145), the following equation for the coefficient of ε^0 is obtained:

$$-\eta_0\omega^2 \sin \phi+\eta_0\omega^2 \sin \phi=0 \tag{149}$$

This equation is always satisfied under the conditions of Eq. (147), and agrees with Eq. (139) which was obtained by neglecting $f_V(t)$.

For the coefficient of ε^1 the following equation can be obtained:

$$\omega^2 u_{1\phi\phi}+\gamma^2 u_{1\sigma\sigma}+\Omega^2 u_{1\tau\tau}+2\gamma\Omega u_{1\sigma\tau}+2\gamma\omega u_{1\sigma\phi}+2\gamma\omega u_{1\tau\phi}+\omega^2 u_1$$
$$=\omega^2(\eta_0 \sin\phi+U\sin\tau)\sin\sigma-2\omega A_1\cos\phi+2B_1\eta_0\omega\sin\phi. \quad (150)$$

The application of the condition of Eq. (148) to Eq. (150) gives

$$A_1=0\ ,\quad B_1=0. \quad (151)$$

Consequently the solution of u_1 is given by

$$u_1=\frac{\eta_0\omega^2}{2\gamma(2\omega+\gamma)}\cos(\phi+\sigma)$$
$$+\frac{\eta_0\omega^2}{2\gamma(2\omega-\gamma)}\cos(\phi-\sigma)$$
$$-\frac{U\omega^2}{2\{\omega^2-(\gamma+\Omega)^2\}}\cos(\tau+\sigma)$$
$$+\frac{U\omega^2}{2\{\omega^2-(\gamma-\Omega)^2\}}\cos(\tau-\sigma), \quad (152)$$

where $\gamma\neq 2\omega$, $\omega\neq\gamma+\Omega$ and $\omega\neq|\gamma-\Omega|$.

As for the coefficients of ε^2, the following equation can be obtained:

$$\omega^2 u_{2\phi\phi}+\gamma^2 u_{2\sigma\sigma}+\Omega^2 u_{2\tau\tau}+2\omega\gamma u_{2\phi\sigma}+2\omega\Omega u_{2\phi\tau}+2\gamma\Omega u_{2\sigma\tau}+\omega^2 u_2$$
$$=\omega^2 u_1\sin\sigma-2\omega A_2\cos\phi+2\omega\eta_0 B_2\sin\phi. \quad (153)$$

The substitution of Eq. (152) into Eq. (153) gives

$$\omega^2 u_{2\phi\phi}+\gamma^2 u_{2\sigma\sigma}+\Omega^2 u_{2\tau\tau}+2\omega\gamma u_{2\phi\sigma}+2\omega\Omega u_{2\phi\tau}+2\gamma\omega u_{2\sigma\tau}+\omega^2 u_2$$
$$=\frac{\eta_0\omega^4}{4\gamma(2\omega+\gamma)}\sin(\phi+2\sigma)-\frac{\eta_0\omega^4}{4\gamma(2\omega-\gamma)}\sin(\phi-2\sigma)$$
$$+\frac{\eta_0\omega^4}{2(2\omega+\gamma)(2\omega-\gamma)}\sin\phi-\frac{U^2\omega^4}{4\{\omega^2-(\gamma+\Omega)^2\}}\sin(\tau+2\sigma)$$
$$+\frac{U\omega^4}{4}\left\{\frac{1}{\omega^2-(\gamma+\Omega)^2}+\frac{1}{\omega^2-(\gamma-\Omega)^2}\right\}\sin\tau$$
$$-\frac{U\omega^4}{4\{\omega^2-(\gamma-\Omega)^2\}}\sin(\tau-2\sigma)$$
$$-2\omega A_2\cos\phi+2\omega\eta_0 B_2\sin\phi. \quad (154)$$

From Eq. (148), we have

$$A_2=0,\quad B_2=-\frac{\omega^3}{4\{4\omega^2-\gamma^2\}} \quad (155)$$

and u_2 is obtained as follows:

$$u_2=-\frac{\eta_0\omega^4\sin(\phi+2\sigma)}{16\gamma^2(2\omega+\gamma)(\omega+\gamma)}-\frac{\eta_0\omega^4\sin(\phi-2\sigma)}{16\gamma^2(2\omega-\gamma)(\omega-\gamma)}$$
$$-\frac{U\omega^4\sin(\tau+2\sigma)}{4\{\omega^2-(\gamma+\Omega)^2\}\{\omega^2-(2\gamma+\Omega)^2\}}$$
$$+\frac{U\omega^4}{4(\omega^2-\Omega^2)}\left\{\frac{1}{\omega^2-(\gamma+\Omega)^2}+\frac{1}{\omega^2-(\gamma-\Omega)^2}\right\}\sin\tau$$
$$-\frac{U\omega^4\sin(\tau-2\sigma)}{4\{\omega^2-(\gamma-\Omega)^2\}\{\omega^2-(2\gamma-\Omega)^2\}}, \quad (156)$$

where $\gamma \neq \omega$, $\omega \neq 2\gamma+\Omega$ and $\omega \neq |2\gamma-\Omega|$.
If the terms of higher order than ε^2 are omitted, $S(t)$, $d\eta_0/dt$ and $d\phi/dt$ are given as follows:

$$\begin{aligned} S(t) = {} & \eta_0 \sin\phi + \varepsilon\omega^2\Big[\frac{\eta_0}{2\gamma(2\omega+\gamma)}\cos(\phi+\gamma t) \\ & + \frac{\eta_0}{2\gamma(2\omega-\gamma)}\cos(\phi-\gamma t) - \frac{U\cos(\gamma+\Omega)t}{2\{\omega^2-(\gamma+\Omega)^2\}} \\ & + \frac{U\cos(\gamma-\Omega)t}{2\{\omega^2-(\gamma-\Omega)^2\}}\Big] + \varepsilon^2\omega^4\Big[-\frac{\eta_0\sin(\phi+2\gamma t)}{16\gamma^2(2\omega+\gamma)(\omega+\gamma)} \\ & - \frac{\eta_0\sin(\phi-2\gamma t)}{16\gamma^2(2\omega-\gamma)(\omega-\gamma)} - \frac{U\sin(\Omega+2\gamma)t}{4\{\omega^2-(\gamma+\Omega)^2\}\{\omega^2-(2\gamma+\Omega)^2\}} \\ & + \frac{U}{4(\omega^2-\Omega^2)}\Big\{\frac{1}{\omega^2-(\gamma+\Omega)^2}+\frac{1}{\omega^2-(\gamma-\Omega)^2}\Big\}\sin\Omega t \\ & - \frac{U\sin(\Omega-2\gamma)t}{4\{\omega^2-(\gamma-\Omega)^2\}\{\omega^2-(2\gamma-\Omega)^2\}}\Big] \end{aligned} \tag{157}$$

$$\frac{d\eta_0}{dt}=0, \tag{158}$$

$$\frac{d\phi}{dt}=\omega\Big[1-\frac{\varepsilon^2}{4\{4-\gamma^2/\omega^2\}}\Big]. \tag{159}$$

Though these equations are derived under the condition that no resonant phenomena appear, some characteristic properties of the true solution of $S(t)$ can be drawn from the approximate solution of the second order.
They are:

a) If ε is appropriately small, and $S(t)$ is obtained up to a proper order, it is possible that $S(t)$ be calculated with some accuracy by the approximate solution except for points of resonance.

b) If any condition of $\omega=\gamma+\Omega$, $\omega=2\gamma+\Omega$, $\omega=|\gamma-\Omega|$, $\omega=|2\gamma-\Omega|$, $\gamma=\omega$ or $\gamma=2\omega$ is satisfied, $S(t)$ becomes infinitely large.
Consequently, $S(t)$ may resonate at these points. Other resonance conditions may appear if we take higher order approximation than ε^2.

c) Since $\frac{d\eta_0}{dt}=0$, η_0 does not increase or decrease with time except at the points of resonance. This implies that $S(t)$ follows harmonic oscillation.

d) Referring to Eq. (159), the natural angular frequency $d\phi/dt$ may be shifted away from ω by the existence of the vertical movement. If $\varepsilon=0.1$ and $\gamma/\omega=1$, the natural frequency becomes

$$\frac{d\phi}{dt}=0.992\omega. \tag{160}$$

The shift of the natural frequency is very small. Therefore, it may be negligible except the neighborhood of $\gamma=2\omega$.

As we mentioned in b), the resonant oscillation may appear if $\gamma=2\omega$, $\gamma=\omega$, $\omega=\gamma+\Omega$, $\omega=2\gamma+\Omega$, $\omega=|\gamma-\Omega|$ or $\omega=|2\gamma-\Omega|$. Since the resonance in the lower modes is more effective, as previously shown, we investigate the behavior of $S(t)$ at $\gamma=2\omega$ and $\omega=|\gamma-\Omega|$.

The homogeneous equation which is derived by using $E=0$ in Eq. (143) is called the Mathieu equation:

$$S''(t)+\omega^2\{1-\varepsilon\sin\gamma t\}S(t)=0. \tag{161}$$

The Mathieu function, which is a solution of Eq. (161), shows the following properties near $\gamma=2\omega$[19].

a) If γ exist inside the region of

$$2\omega\left[1-\frac{\varepsilon}{4}-\frac{\varepsilon^2}{64}\right]<\gamma<2\omega\left[1+\frac{\varepsilon}{4}-\frac{\varepsilon^2}{64}\cdots\cdots\right], \tag{162}$$

then $S(t)$ becomes unstable and increases exponentially as t becomes large. $\gamma=2\omega$ is the condition of a resonance, which is called the parametric resonance and occurs if $\frac{2\omega}{\gamma}=n$, where n is positive integer.

b) At $\gamma=2\omega\left[1\pm\frac{\varepsilon}{4}-\frac{\varepsilon^2}{64}\cdots\right]$, $S(t)$ has two independent solutions: one is a periodic function and the other is non-periodic function which increases with t.

c) If γ is outside the region defined in a), $S(t)$ becomes stable and the amplitude of $S(t)$ is finite for any value of t.

Furthermore, we investigate the resonance at $\omega=(\Omega-\gamma)$. In resonant phenomena, the phase difference between the resonance and external force, as well as the amplitude of the fundamental mode, is very important. This difference is represented as folllows:

$$\nu=\psi-(\Omega-\gamma)t, \tag{163}$$

where ψ is a phase of $S(t)$, and ν is a phase difference.

It is assumed that the amplitude η_0 and the phase ψ can be expanded, as previously, into power series of ε:

$$\frac{d\eta_0}{dt}=\varepsilon A_1(\eta_0,\nu)+\varepsilon^2 A_2(\eta_0,\nu)+\cdots\cdots, \tag{164}$$

$$\frac{d\psi}{dt}=(\Omega-\gamma)+\varepsilon B_1(\eta_0,\nu)+\varepsilon^2 B_2(\eta_0,\nu)+\cdots\cdots, \tag{165}$$

and $S(t)$ is also assumed to be expanded into a power series of ε:

$$S(t)=\eta_0\sin(\lambda+\nu)+\varepsilon u_1(\eta_0,\nu,\lambda,\mu)+\varepsilon^2 u_2(\eta_0,\nu,\lambda,\mu)+\cdots\cdots\cdots\cdots\cdots\cdots\cdots. \tag{166}$$

where, $\lambda=(\Omega-\gamma)t$, and $\mu=(\Omega+\gamma)t$.

We assume that ω^2 is different from $(\Omega-\gamma)^2$ by $\varepsilon\Delta$:

$$\omega^2=(\Omega-\gamma)^2+\varepsilon\Delta. \tag{167}$$

By substituting these equations into Eq. (145), approximate solutions can be obtained. We calculate the first approximate solution. The first order equation gives

$$\left.\begin{aligned} A_1&=\frac{(\Omega-\gamma)U}{4} \\ B_1&=\frac{\Delta}{2(\Omega-\gamma)} \end{aligned}\right\} \tag{168}$$

Then:

$$\frac{d\eta_0}{dt}=\varepsilon\frac{(\Omega-\gamma)U}{4}, \tag{169}$$

$$\frac{d\psi}{dt}=(\Omega-\gamma)+\frac{\Delta\varepsilon}{2(\Omega-\gamma)}. \tag{170}$$

Equation (169) and (170) imply that the amplitude of the fundamental mode increases and the phase difference becomes large.

When the higher order approximation is applied, the resonance is

$$\omega=|n\gamma-\Omega|, \tag{171}$$

where n is an arbitrary positive integer.

At these points the behavior of $S(t)$ is the same as in the case of $\omega=(\Omega-\gamma)$. The occurrence of the resonant phenomena of Eq. (171) in the presence of vertical movement means that even if γ and Ω have large values, such as those of an earthquake, resonant phenomena in lower natural frequencies may appear. This is of great importance in the design of oil storage tanks, since it indicates that vertical movement plays a major role in the resonant phenomena of tanks.

This conclusion is also applicable to the corresponding phenomena inside a ground storage tank.

7. Equipment and Experimental Procedure

(1) Model tanks and wave channel

Since we did not have model tank with which the experiments for two different liquids could be carried out, tanks which were partially filled with water were used for the evaluation of the theory derived in the previous chapter.

In the experiments, two kinds of tanks were used: one was a steel-made circular tank with an inner radius of 45cm and a height of 80cm, and the other was an acrylic rectangular tank with a length of 100cm, a width of 50cm and a height of 40cm. Since the theory is applicable to the computation of propagating wave heights generated by a piston type wave generator, a wave channel with such a generator was used. The channel, shown in **Fig. 5**, has a length of 40 m, a height of 1.5 m and a width of 2.0m near the wave paddle, gradually reducing to 1.5m, 7.0m away.

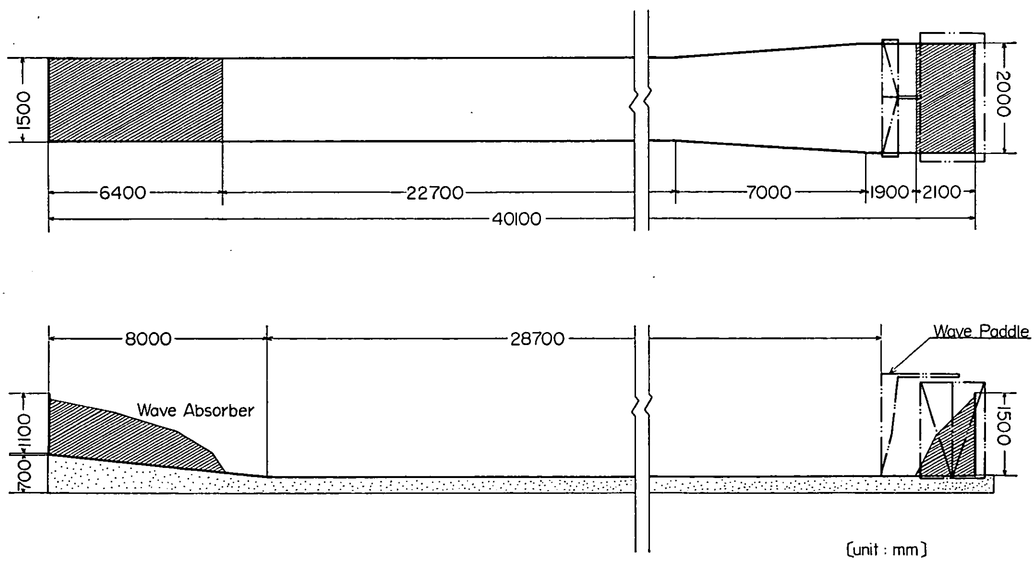

Fig. 5 Wave Channel

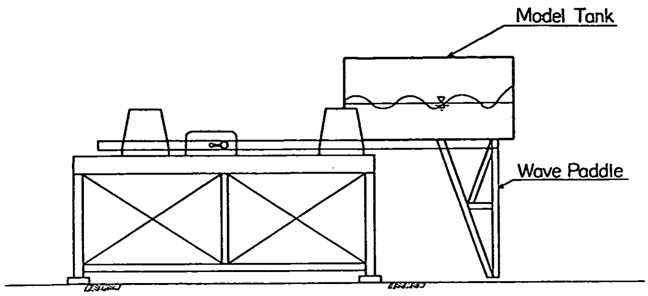

Fig. 6 Wave Generator, and Wave Paddle with Tank

Both kinds of tanks were clamped on to the top of the wave paddle so as to move with it. **Figure 6** shows the wave generator and a tank fixed to the wave paddle. **Photographs 1** and 2 show the fixed rectangular and circular tanks.

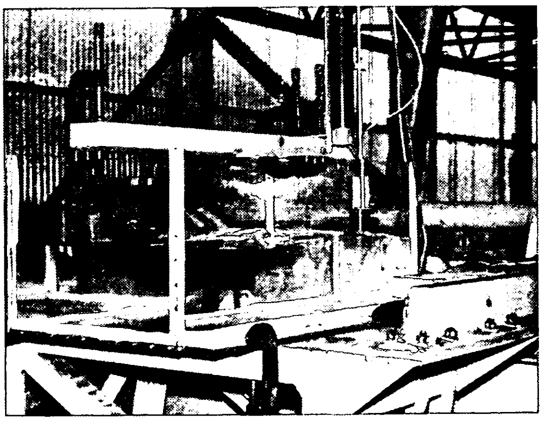

Photo. 1 Rectangular Tank Arrangement

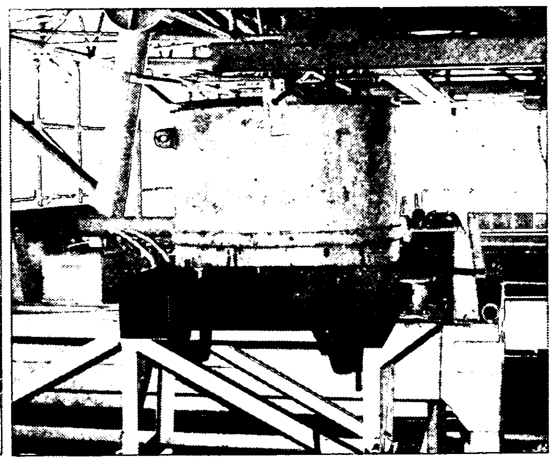

Photo. 2 Circular Tank Arrangement

(2) Mechanism of the wave paddle movement

A low frequency signal generator was used as the generator of input signals to a wave generator control system. Though the low frequency signal generator can produce three kinds of periodic signals such as sinusoidal waves, triangular waves, and rectangular waves, only sinusoidal waves were used for the experiments. A special DC motor, having very little inertia, rotates according to the signals received from the wave generator control system, and the rotation is transformed to fore-and-aft movements of the wave paddle by a cylindrical screw bar. **Photograph 3** shows the wave generator.

(3) Wave Measuring and recording equipment

The waves developed in the tanks or the channel were measured by capacitance type wave gauges, as shown in **Photo. 4**. The out-put signals from the wave gauges were amplified, and recorded on magnetic tapes by a data recorder. At the same time, they were drawn by a pen recorder.

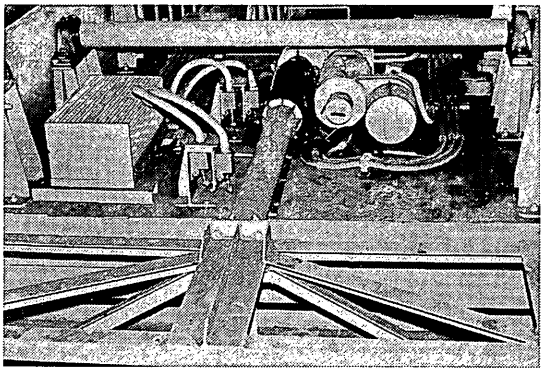

Phto. 3 Wave Generator

The displacement of the wave paddle was measured by a displacement meter, which is shown in **Photo. 5**. The displacement was also recorded in the same way as the waves.

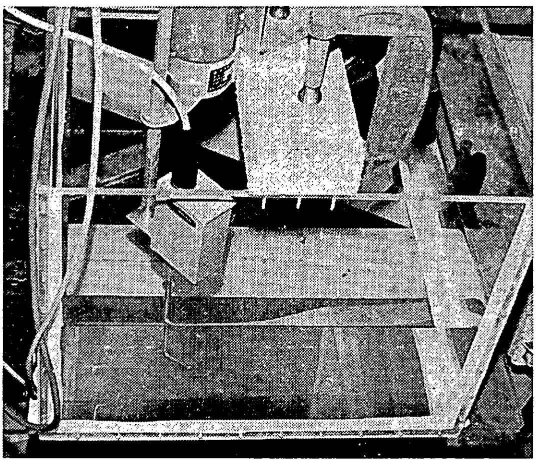

Photo. 4 Capacitance Type Wave Meter

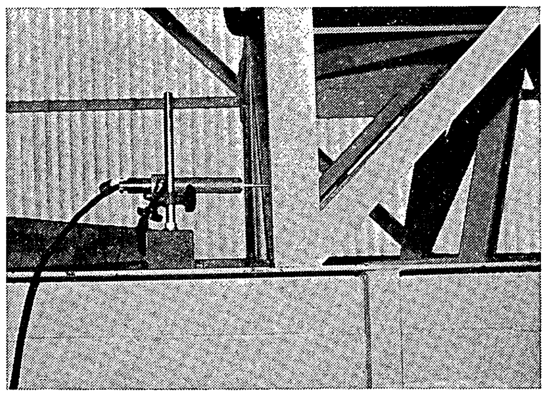

Photo. 5 Displacement Meter

(4) Experimental conditions and method of analysis

The water depth was set at 40cm in the circular tank, 20cm in the rectangular tank, and 40cm and 70cm in the wave channel. The experiments for both tanks were carried out in the tank movement frequency range of 0.7 to 3.0cps. Also frequencies up to 4.0cps were added for the experiments on the rectangular tank. The positions of a wave gauge in the tanks are shown in **Fig. 7** and 8. The longitudinal axis of the rectangular tank is parallel to the movement direction.

The experiments in the wave channel were performed at three frequencies, 0.5, 1.0 and 1.5cps, for each water depth. Three wave gauges were set at 0.065m, 10m, and 15m from the front of the wave paddle.

The amplitudes of the wave paddle displacement were aimed to be 1/100 of the water depth in each experiment, but their values showed some variation for each frequency. The small amplitudes were taken to satisfy the wave linearity.

The analog data of the water surface and wave paddle displacements, which were recorded on analog magnetic tapes, were converted into digital data at an appropriate time intervals by a high speed A/D converter.

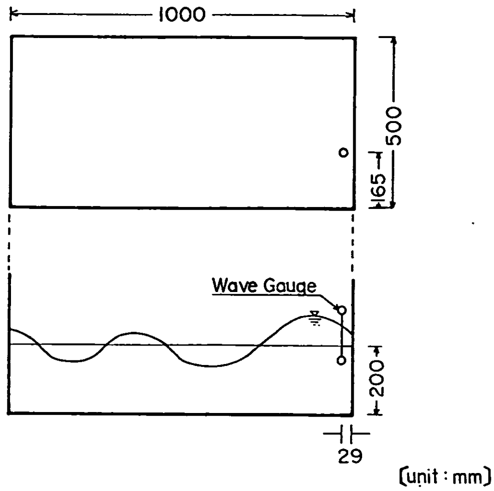

Fig. 7 Position of the Wave Gauge in the Rectangular Tank

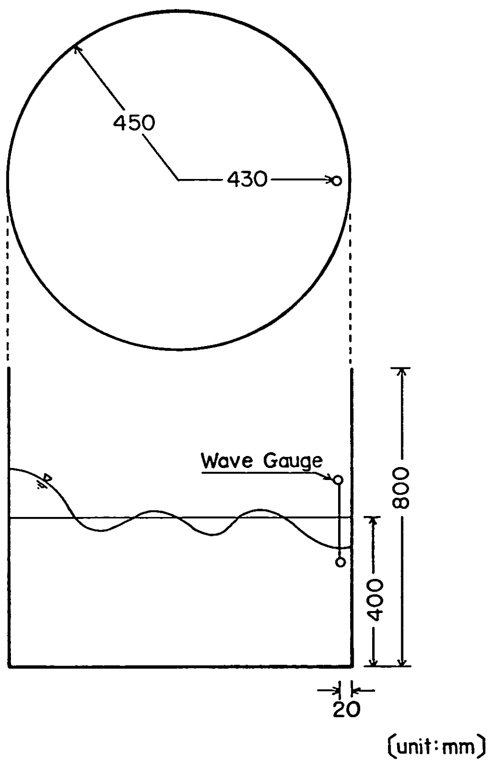

Fig. 8 Position of Wave Gauge in the Circular Tank

The converted digital data of the paddle displacement were used as input data, for a TOSBAC 5600 digital computer in the Port and Harbour Research Institute, in order to compute the theoretical formula. The digital wave data were used for drawing the figures of the water surface displacement.

The figures of the computed and the measured water surface displacements were drawn by an automatic drafting system in the Institute.

8. Experimental Results and Discussion

Since in the experiments the tanks were forced to move only horizontally and the fluid in the upper layer is air, of which density is small enough to be negligible, the water surface displacement is computed by taking ρ_{I} and $f_V''(t)$ in Eqs. (80) and (125) as zero.

8.1 Rectangular Tanks

Table 1 shows the resonant frequencies of the water surface in the rectangular tank with a

Table 1 Natural Frequencies of the Fluid in the Rectangular Tank (l_x=1.0m, l_y=0.5m, h=0.2m)

n	1	3	5	7	9	11	13	15	17	19	21
f_n(cps)	0.659	1.495	1.971	2.336	2.649	2.972	3.184	3.420	3.641	3.843	4.047

water depth at 0.20m. In the rectangular tank even number modes cannot exist, which is evident from Eq. (80) or (81).

Figures 9 to **14** show the comparison of the computed values to the experimental values of the water surface elevation, for each frequency. In each figure, a solid line, small circles and a dashed line denote the theoretical curve, experimental values, and the wave paddle displacement, respectively. In the figures, the paddle displacement shows an approximate sinusoidal curve which is flattened near peaks and troughs rather than a perfect sinusoidal curve. The center line of the wave paddle displacement initialy shifts rapidly and then keeps its position constant. Due to this fact, the theoretical water surface displacement computed by a sinusoidal displacement could not be compared with that of the experiments. Therefore, the measured paddle displacement was used for the theoretical computation.

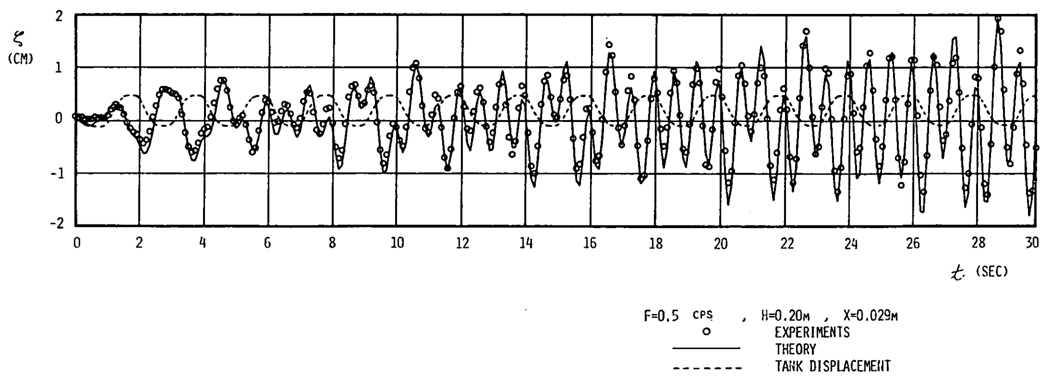

Fig. 9 Theoretical and Experimental Wave Profile in the Rectangular Tank, f=0.5cps

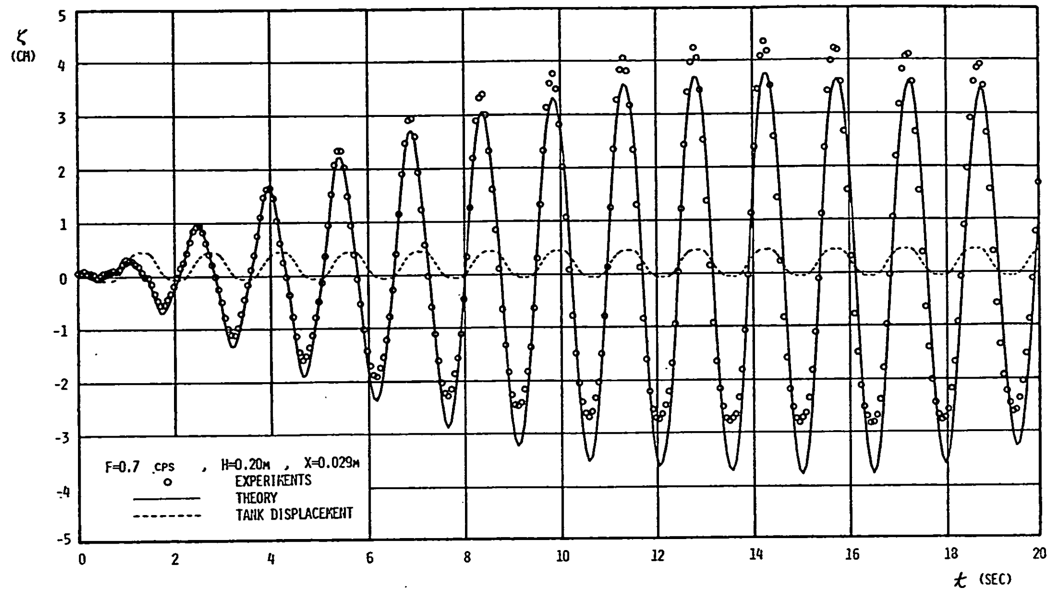

Fig. 10 Theoretical and Experimental Wave Profile in the Rectangular Tank, f=0.7 cps

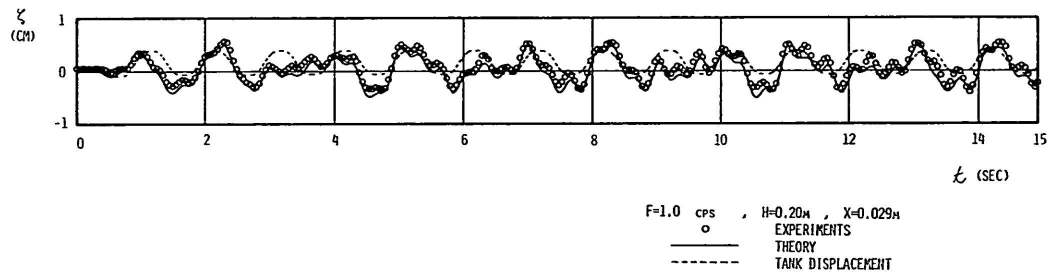

Fig. 11 Theoretical and Experimental Wave Profile in the Rectangular Tank, f=1.0 cps

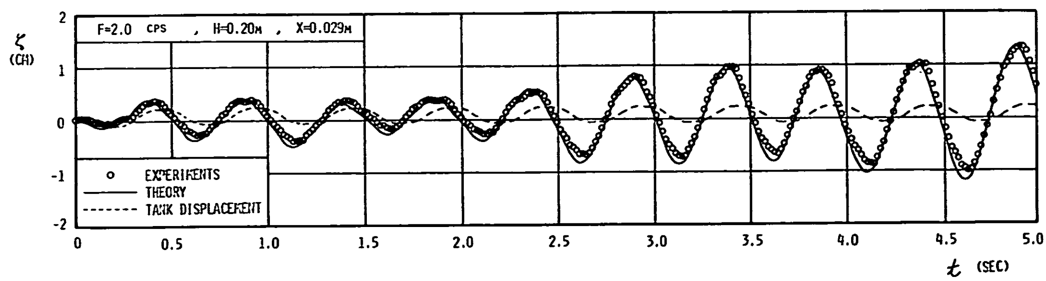

Fig. 12 Theoretical and Experimental Wave Profile in the Rectangular Tank, f=2.0 cps

In **Fig. 9**, f=0.5cps, which is smaller than the natural frequency of the first mode, the water surface displacement is initialy in phase with the tank movement but becomes out of phase as time passes. The theoretical curve agrees quite well with the experimental values.

In **Fig. 10**, the water surface displacement is greatly inreased, because f=0.7cps is near the natural frequency of the first mode which is f=0.659cps. The water surface displacement

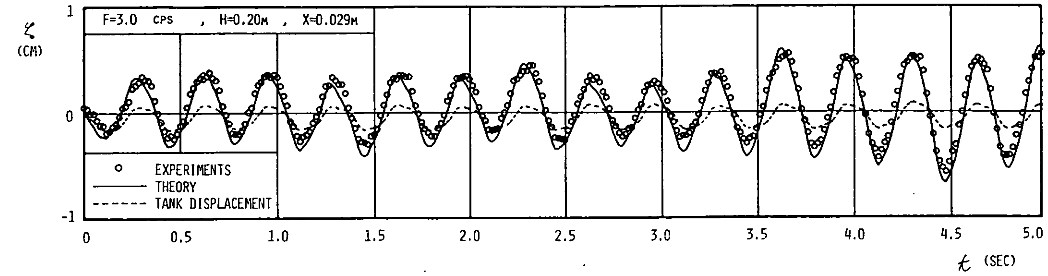

Fig. 13 Theoretical and Experimental Wave Profile in the Rectangular Tank, f=3.0cps

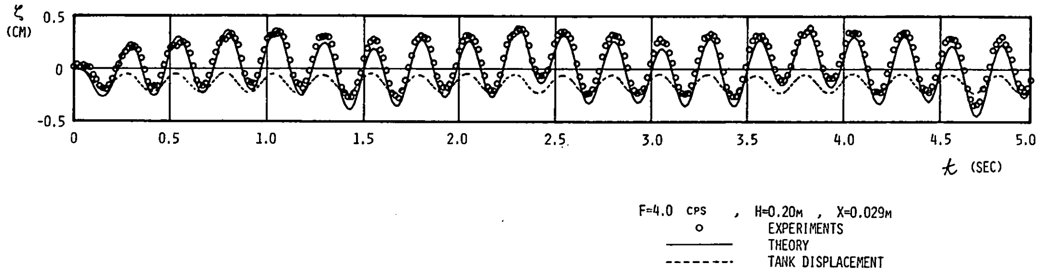

Fig. 14 Theoretical and Experimental Wave Profile in the Rectangular Tank, f=4.0cps

becomes almost in phase with the tank displacement but is more than 10 times larger near maxima or minima. At the maxima, the experimental values are 1.1 times as large as the theoretical values, and at the minima, the former is 0.8 times as small as the latter. It is believed that these discrepancies are caused by the effect of wave nonlinearity. The theory, however, well represents the actual water surface behavior.

Since for the other frequencies the water surface displacement is not large, the nonlinear effect does not appear and the theoretical curve shows a good agreement with experimental values. Though f=2.0cps (**Fig. 12**) is near the natural frequency of the third mode, f=1.97 cps, the water surface displacement is not as amplified as in the case of f=0.7cps (**Fig. 10.**) The reason for the small amplification was previously mentioned in **6.1**.

Since in these experiments the durations of tank oscillations were shorter than one minute, and the amplitude of the tank displacements were kept small, the cross waves reported by Sawamoto and Kato[17] were not developed inside the rectangular tank. The standing waves of high frequency, however, were observed over the width of the tank, when the frequency of the tank displacement was higher than 2.0 cps. The time of the standing waves' appearance was not constant, and appeared earlier as the frequency increased. For example, in the case of f=2.0cps, the standing waves began to appear after 25 seconds. The causes of the standing waves are unknown since the analysis of the data is finished before their appearance.

8.2 Circular Tanks

Table 2 shows the natural resonant frequencies of the circular tank with the water depth of 40cm.

Figures 15 to **19** show the comparison of the theoretical curve to the experimental values. We note that f=0.5cps (**Fig. 15**) and f=0.7cps (**Fig. 16**) are cases of smaller frequencies than that of the first mode, f=0.970 cps.

Table 2 Natural Frequencies of the Fluid in the Circular Tank (r_0=0.45m, h=0.4m)

i	1	2	3	4	5	6
f_n(cps)	0.970	1.715	2.170	2.541	2.863	3.152

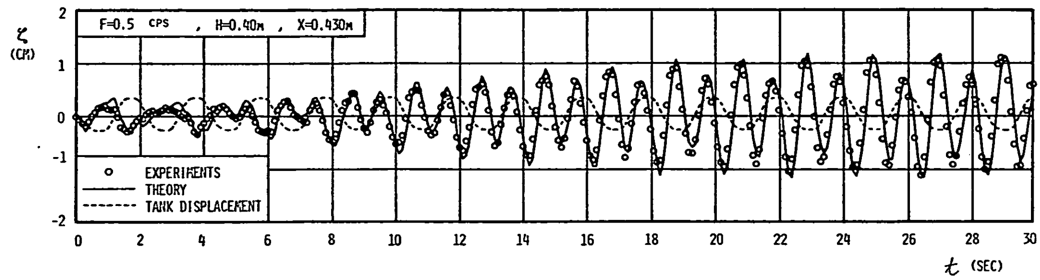

Fig. 15 Theoretical and Experimental Wave Profile in the Circular Tank, f=0.5 cps

The water surface displacement for f=0.7 cps is larger than that of 0.5 cps, because f=0.7 cps is nearer to the natural frequency of the first mode.

When f=1.0cps which is nearest to the natural frequency of the first mode, the water surface displacement gradually increases with time (see **Fig. 17**). The effect of the natural frequency becomes so remarkable that the effects of the other modes disappear. When the frequencies of the tank oscillation are as large as f=3.0 cps, the disagreement between the theoretical curve and the experimental values becomes noticeable.

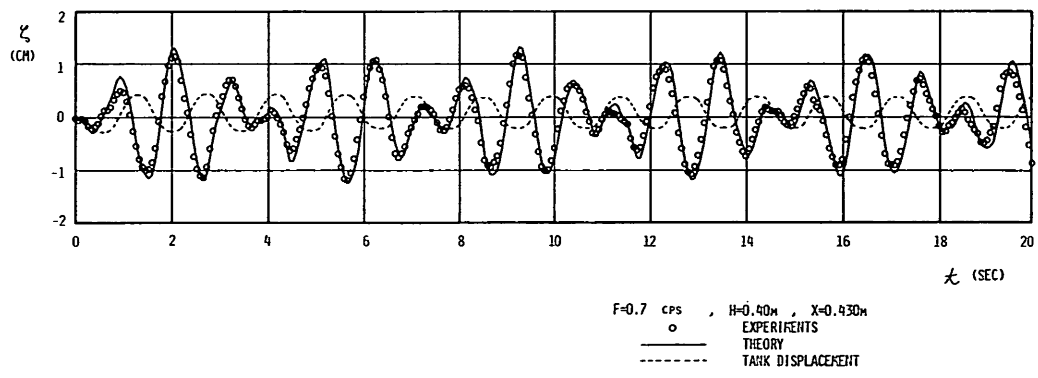

Fig. 16 Theoretical and Experimental Wave Profile in the Circular Tank, f=0.7 cps

We believe that the following are the causes of that disagreement:

a) The nonlinear effect increases in higher frequencies.

b) Quite different phenomena, such as cross waves which travell along the wall of the tank, as reported by Shiigai and Ishikawa[16], may have developed. They could not be observed because the water surface behavior was not visible from the outside of the tank.

Though **Figs. 15** to **19** show small discrepancies in some area, it is not an overstatement to say that the theoretical curves agree quite well with the experimental values.

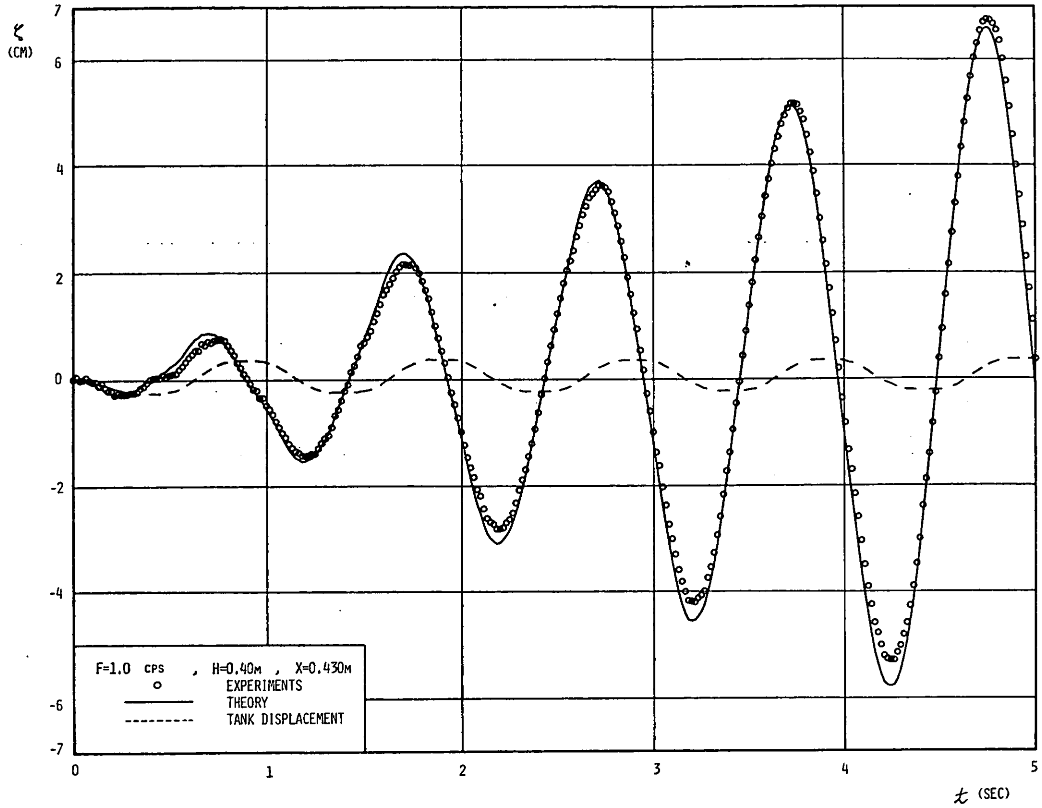

Fig. 17 Theoretical and Experimental Wave Profile in the Circular Tank, f=1.0 cps

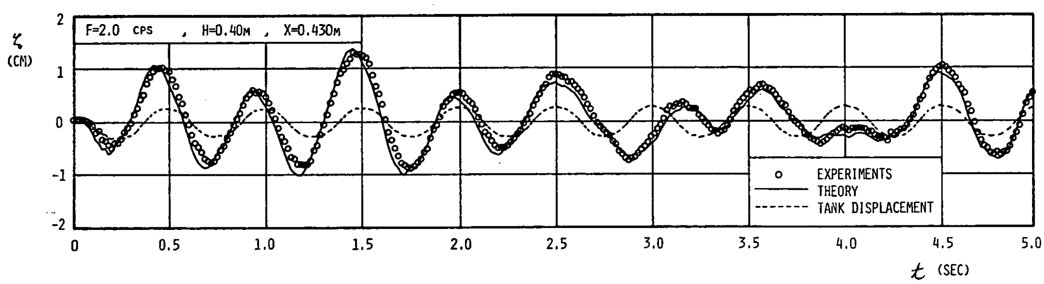

Fig. 18 Theoretical and Experimental Wave Profile in the Circular Tank, f=2.0 cps

8.3 Wave Propagation in a Channel

The solution for a rectangular tank is applicable to the computation of propagating waves generated by a piston type wave paddle, if the length of the tank is assumed to be sufficiently long. If the length is short, in the computation the waves generated at the side wall of the tank are, within a short time, superposed by the waves generated at the opposite side wall and therefore do not represent the actual propagating waves generated by a wave paddle. Taking into account computation time of the solution, the necessary length of a rectangular tank was determined to be 100m.

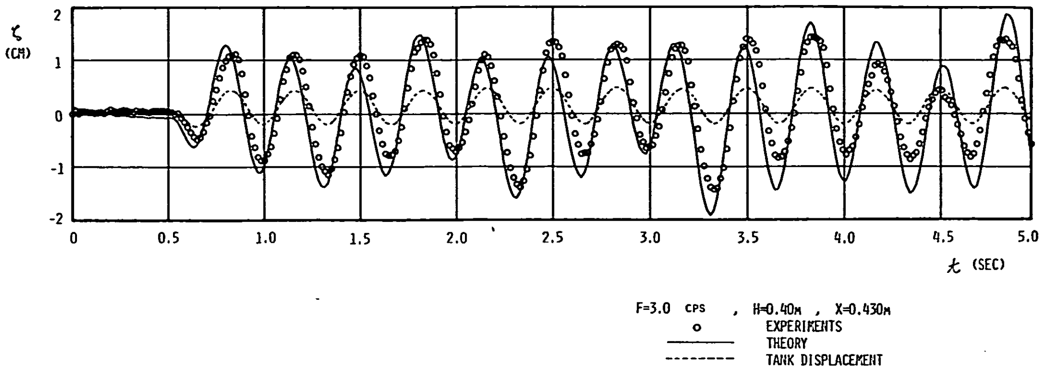

Fig. 19 Theoretical and Experimental Wave Profile in the Circular Tank, f=3.0 cps

In the case of the water depth at 0.70 m, the wave cellerity of a long wave is 6.28 m/sec. It takes about 32sec for the long wave to travel to the point of 85m away from the wall. Therefore, if the computation of wave heights is stopped within the time, the computed waves at a point 15m away from the wall are not supposed to be influenced by the waves from the opposite side. The computations of the propagating waves were performed by taking the measured wave paddle displacement as input data.

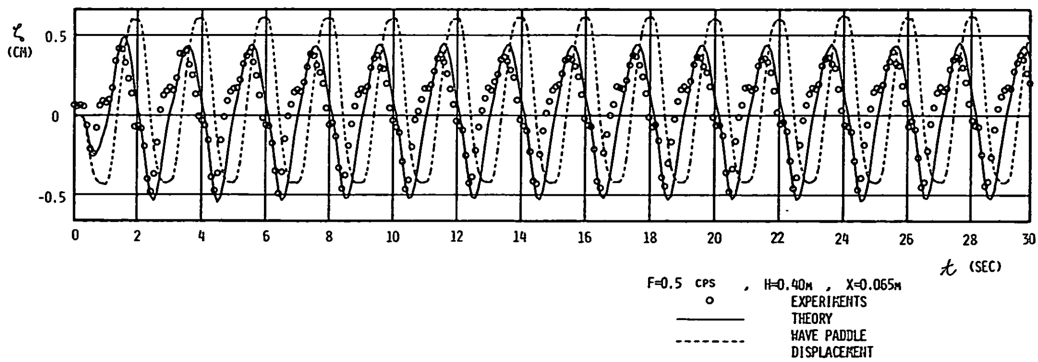

Fig. 20 (a) Theoretical and Experimental Values of Wave Propagation in the Wave Channel, h=0.4m, f=0.5 cps, x=0.065m

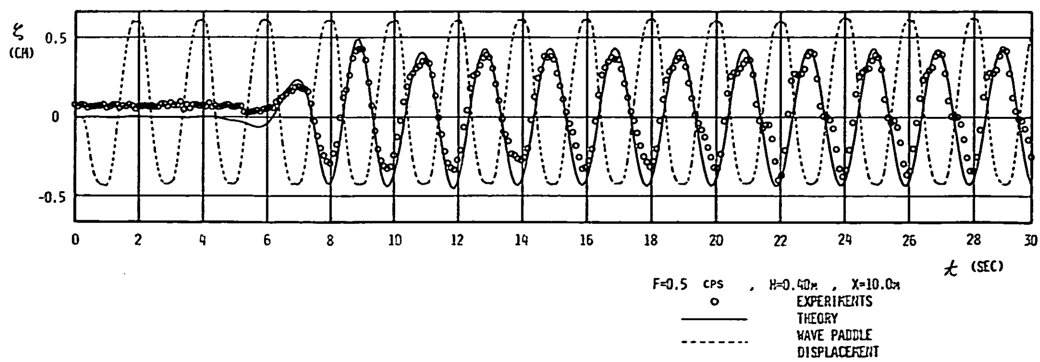

Fig. 20 (b) Theoretical and Experimental Values of Wave Propagation in the Wave Channel, h=0.4m, f=0.5 cps, x=10.0m

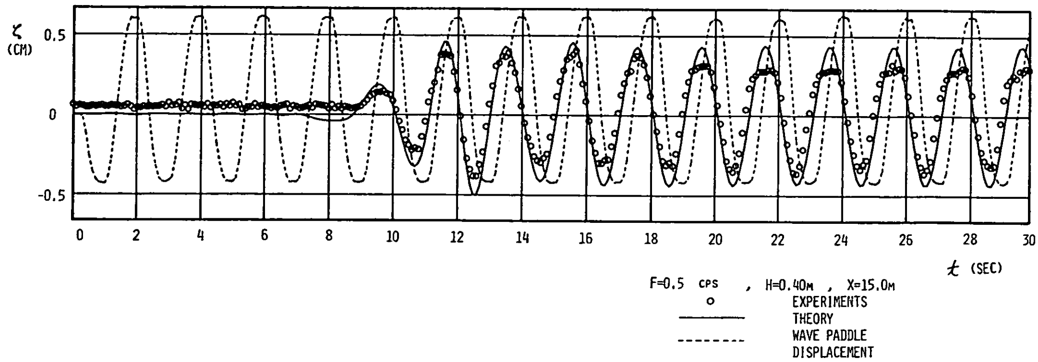

Fig. 20 (c) Theoretical and Experimental Values of Wave Propagation in the Wave Channel, h=0.4m, f=0.5 cps, x=15.0m

Figures 20 to **23**, for example, show the comparison of the computed waves with the experimental waves. In the experiments, wave gauges were set at points 0.065m, 10m, and 15m away from the wave paddle. **Figure 20** is the case of wave paddle frequency of f=0.5cps and water depth of 0.4m, **Fig. 20 (a)**, for x=0.065m in front of the waves paddle, the computed wave heights agree well with experimental ones; the computed wave shapes slightly differ from the experimental ones about the wave fronts. In **Fig. 20 (b)**, for x=10m, and **Fig. 20 (c)**, for x=15m, the theory represents the true state of the wave propagation; first, long waves of small amplitudes formed, followed by shorter waves of higher amplitudes, and finally waves of constant period and amplitude arrive. The computed wave shapes also show a good agreement with the experimental ones.

Figure 21, for f=0.5cps and water depth of 0.7m, shows a good agreement on the whole, between the experiments and the theory, though the computed values at the wave troughs are 1.2 times as large as the experimental values. **Figure 22** and **23** for f=1.5cps also

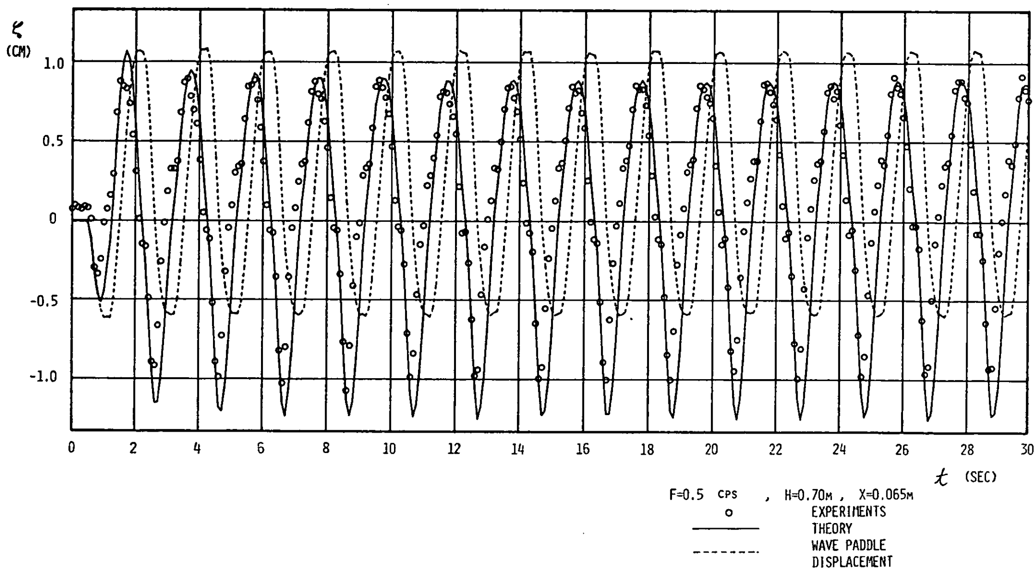

Fig. 21 (a) Theoretical and Experimental Values of Wave Propagation in the Wave Channel, h=0.7m, f=0.5 cps, x=0.065m

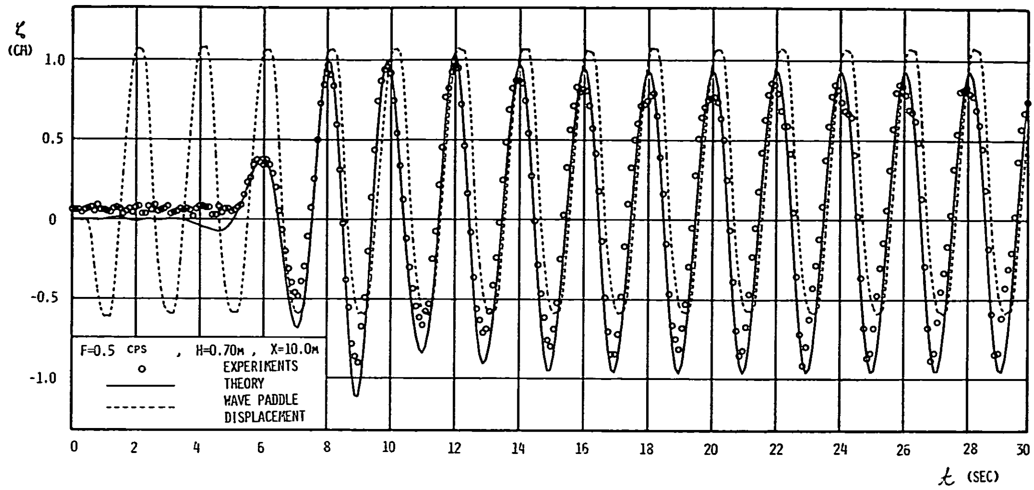

Fig. 21 (b) Theoretical and Experimental Values of Wave Propagation in the Wave Channel, $h=0.7$m, $f=0.5$ cps, $x=10.0$m

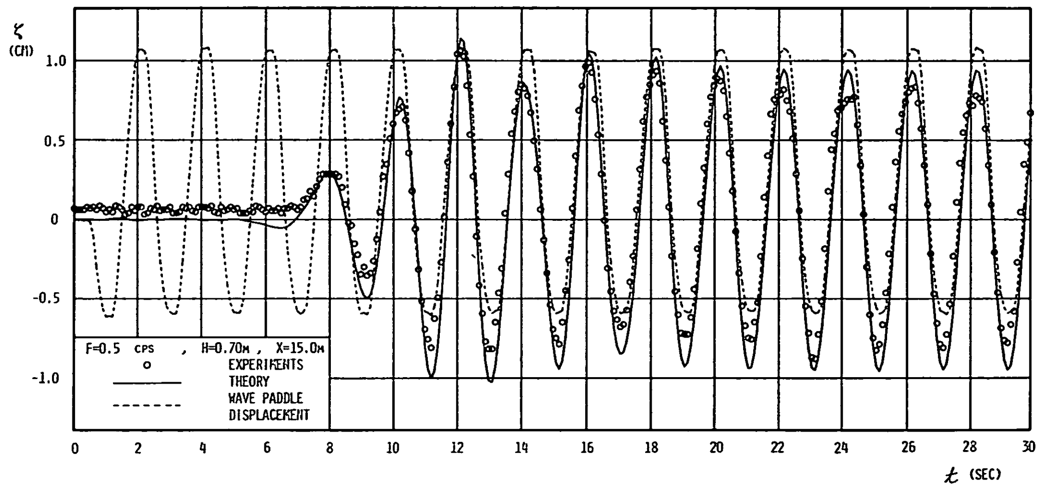

Fig. 21 (c) Theoretical and Experimental Values of Wave Propagation in the Wave Channel, $h=0.7$m, $f=0.5$ cps, $x=15.0$m

show quite close agreement between the theory and the experiments.

Whenever we measure the wave heights at a point away from the wave paddle, we observe the phenomena that first, long waves of small amplitudes reach the gauge and then several higher waves come just before the uniform wave train. In these figures, this phenomena are well shown even by the theory derived from linear equations.

Sverdrup and Munk have given an excellent description of the energy transformation process and presented a computation method for the wave energy distribution in the leading part of wave train[20]. We computed the wave height distribution by their method and compared it to that computed by the author's theory and to that obtained in the experiments. **Figure** 24 shows the distribution of wave heights at $x=10$m. In the figure, ζ_{max} represents

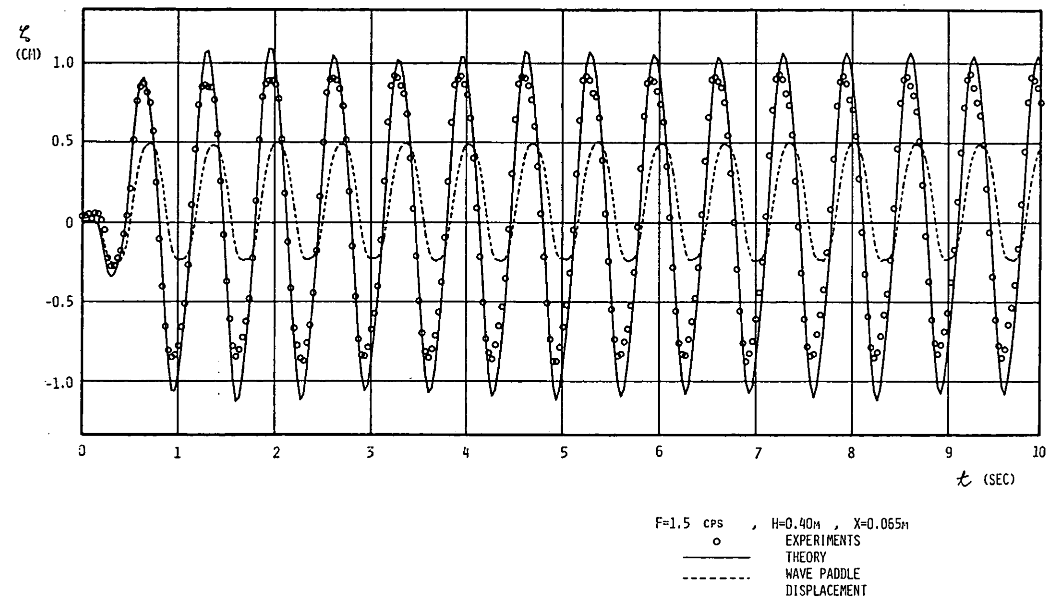

Fig. 22 (a) Theoretical and Experimental Values of Wave Propagation in the Wave Channel, h=0.4m, f=1.5 cps, x=0.065m

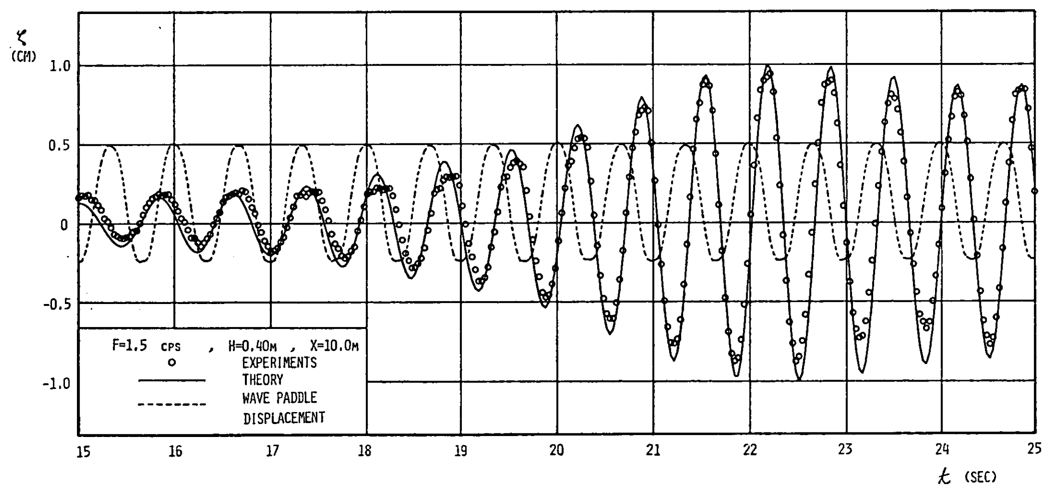

Fig. 22 (b) Theoretical and Experimental Values of Wave Propagation in the Wave Channel, h=0.4m, f=1.5 cps, x=10.0m

the wave height and ζ_0 is wave height of the uniform train.

The computation of the distribution was carried out for the experiments where f=1.5cps and water depth = 0.7m; the waves were deep water waves. The distribution computed by the author's theory agree well with that of the experiments. The distribution curve computed by Sverdrup and Munk's method is, however, different from that of the experiments.

In the author's theory, the waves generated by the wave paddle are taken as a super-

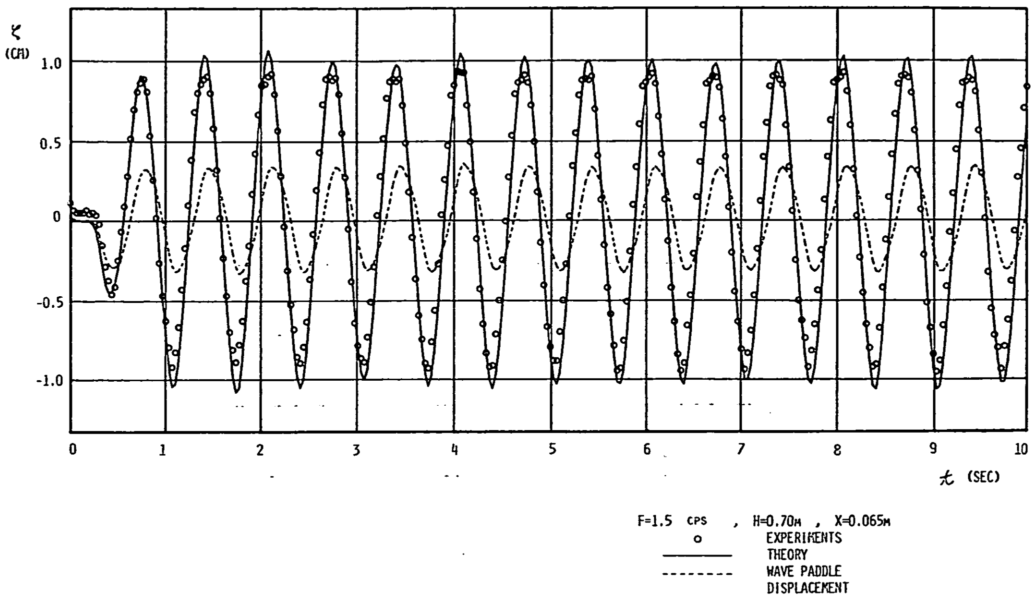

Fig. 23 (a) Theoretical and Experimental Values of Wave Propagation in the Wave Channel, $h=0.7$m, $f=1.5$ cps, $x=0.065$m

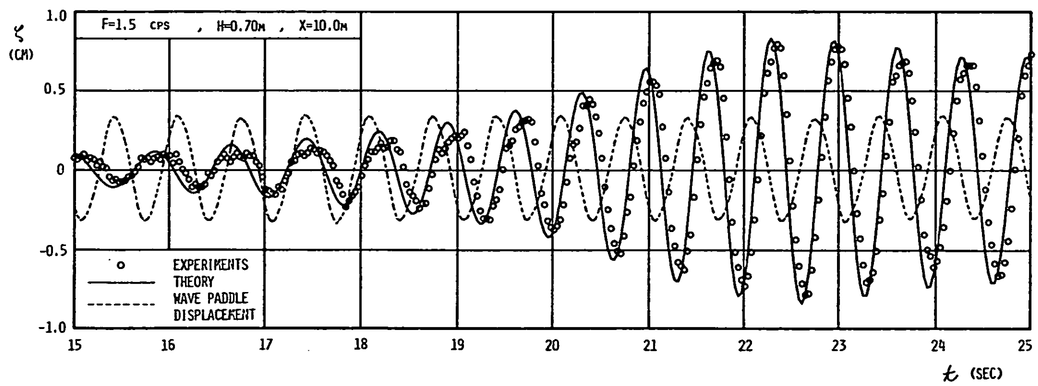

Fig. 23 (b) Theoretical and Experimental Values of Wave Propagation in the Wave Channel, $h=0.7$m, $f=1.5$ cps, $x=10.0$m

position of infinite sinusoidal waves as one can easily understand from Eq. (83). Therefore, the waves are not a single sinusoidal waves as Sverdrup and Munk assumed. Consequently the good agreement of the theory with the experiment implies that even if waves are regular, their propagation properties cannot be truely expressed by a single sinusoidal wave.

Pierson[21] also investigated the propagation of regular waves, by the Fourier integral development of a finite regular wave train, and showed the distribution of the wave heights at an arbitrary point. His analytical method is essentially the same as the author's, since he dealt with the regular wave train as a superposition of an infinite number of sinusoidal component waves.

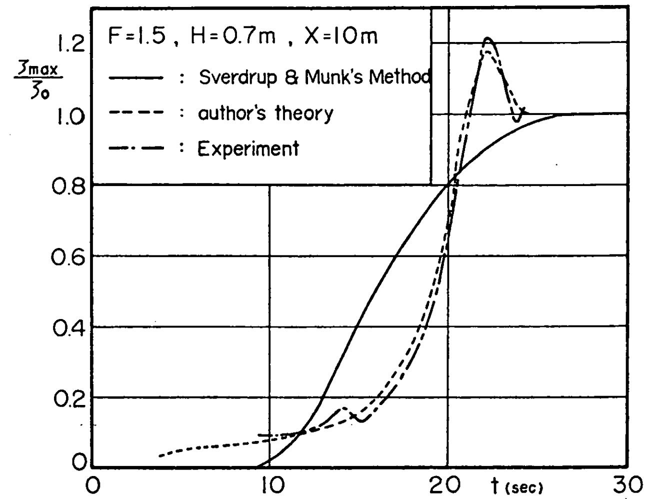

Fig. 24 Wave Height Distribution of the Leading Part of the Wave Train

9. Conclusions

The following major conclusions can be drawn from the study on the excited waves in a transient state:

1. The linearizing conditions are made clear as follows:

   a) The amplitudes of the tank displacement must be very small compared to the tank dimensions and to the thicknesses of the fluid layers,

   b) The acceleration of a fluid particle on the boundary layer must be very small compared to the total gravitational acceleration and vertical accelerations due to the vertical tank movement.

2. The basic differential equations which determine internal wave amplitudes and dynamic fluid pressures in transient state are obtained for rectangular or circular tanks.

3. The basic differential equation is analytically solved when the vertical tank oscillation does not exist. By using the solution of this equation, the internal waves and the dynamic fluid pressure can be computed.

4. Resonant phenomena inside a tank in higher modes have less effect than in lower modes.

5. In the presence of vertical movement, an approximate solution can be derived if there is no resonance. According to the approximate solution, the internal waves resonate under the following conditions:

$$\omega_n = \Omega,$$

$$\omega_n = m\gamma/2,$$

$$\omega_n = |m\gamma + \Omega| \text{ or } \omega_n = |m\gamma - \Omega| \quad (m = 1, 2, 3 \cdots\cdots)$$

where ω_n is the n-th natural angular frequency of the fluids inside the tank, Ω and γ are the angular frequencies of the horizontal and vertical oscillations, respectively.

The behavior of the boundary layer between both fluids is also investigated under resonance conditions.

6. The vertical movement of a tank plays an important role in the resonance of the fluid.
7. The theory is applicable to a ground tank as well as to a sea tank.
8. The validity of the theory was confirmed by the experiments with rectangular and circular tanks which were partially filled with water and vibrated only horizontally.
9. The solution for the rectangular tank can be applied to the problem of wave propagation in a channel, produced by a piston type wave generator. The validity of the solution was confirmed, for the estimation of propagting wave heights, by the experiments in a wave channel.

The following problems remain to be scrutinized:

a) Experimental confirmation of the theory for two different fluid layers.
b) Confirmation of the resonant conditions and performance of the computation for the case of simultaneous vertical and horizontal tank movements.
c) Experimental confirmation of the theoretical pressure.
d) Application method of the theory to practical problems.

These problems will be dealt with in the author's forthcoming paper.

Acknowledgements

The author wishes to express his sincere gratitude to Professor Fredric Raichlen, California Institute of Technology, for his usefull suggestions and discussions on the importance of the transient phenomena inside a tank, offered during the author's study at that Institute.

The author also wishes to thank Dr. Yoshimi Goda, Chief of the Wave Loboratory of the Port and Harbour Research Institute, for his providing for the experiments and for his helpfull discussions during the development of the theoretical analysis of this study.

A special debt of gratitude is owed to Mr. Yutaka Kamiyama, Member of the Wave Laboratory, who assisted the author in performance of the experiments and drafted all figures appearing in this manuscript.

The author also wishes to thank other members of the Wave Laboratory for their temporary assistance in performing the experiments or constructing the model rectangular tank.

(Received on March 31, 1976)

References

1) The Committee of Deep Sea Structure: "Report of Investigation of Deep Sea Structures —Oil Storage Tanks in Offshore Sea—," Corporation of Ocean Industry Investigation, 1976, (*in Japanese*)
2) Nagasu, S.: "Deep Sea Oil Storage Tanks of PS Concrete and their Properties of Water Proof Durability," Journal of Concrete Engineering, Vol. 13, No. 8, 1975, pp. 29–30, (*in Japanese*)
3) Brogren, E. et al: "Field Data Recovery System Khazzan Dubai No. 3," The 6th OTC, Paper No. 1943, 1974
4) Seki, H. and Koga, H.: "Durability of Prestressed Concrete under Marine Environments," Technical Note of the Port and Harbour Research Institute, No. 191, 1974, (in *Japanese*)
5) Westergaard, H.M.: "Water Pressure on Dams during Earthquakes," Transaction of ASCE, Vol. 98, Paper No. 1835, 1933, pp. 418–433
6) Jacobson, L.S.: "Impulsive Hydrodynamics of Fluid inside Cylindrical Tank and of Fluid Surrounding a Cylindrical Pier," Bull. Seism. Soc. Am., Vol. 39, 1934, pp. 189–204
7) Housner, G.W.: "Dynamic Pressures on Accelerated Fluid Containers," Bull. Seism. Soc. Am., Vol. 47, 1957, pp. 15–35
8) Shiraki, M. and Hujita, K.: "Analysis of the Seismic Responses of Self-supported Thin Cylindrical Storage Tanks," Mitsubishi Juko Giho, Vol. 12, No. 3, 1975, pp. 282–294,

(*in Japanese*)
9) Chester, W.: "Resonant Oscillation of Water Waves," Proceedings of Royal Society of London, Vol. 306, 1968, pp. 5-22
10) Faltinsen, O.M.: "A Nonlinear Theory of Sloshing in Rectangular Tanks," Journal of Ship Research, Vol. 18, No. 4, 1974, pp. 224-241
11) Sogabe, K. and Shibata, H.: "Response Analysis on Sloshing of Liquid in a Cylindrical Storage-I—Basic Equation and Response to Sinusoidal Input—," Journal of the Institute of Industrial Science, Vol. 26, No. 3, 1974, pp. 119-122, (*in Japanese*)
12) Sogabe, K. and Shibata, H.: "Response Analysis on Sloshing of Liquid in a Cylindrical Storage-II—Transient Response to Sinusoidal Input-," Journal of Institute of Industrial Science, Vol. 26, No. 4, 1974, pp. 152-154, (*in Japanese*)
13) Sogabe, K. and Shibata, H.: "Response Analysis on Sloshing of Liquid in a Cylindrical Storage-III—A Method of Simple Evaluation of Transient Response to Sinusoidal Input —," Journal of Institute of Industrial Science, Vol. 26, No. 8, 1974, pp. 309-312, (*in Japanese*)
14) Kotsubo, S.: "Dynamic Water Pressure on Dams due to Irregular Earthquakes," Memoirs of the Faculty of Engineering, Kyushu Univerity, Vol. 18, No. 4, 1959, pp. 119-129
15) Wylie, E.B.: "Seismic Response of Reservoir-Dam System," Journal of the Hydraulics Division, ASCE, Vol. 101, No. HY3, 1975, pp. 403-419
16) Ishikawa, T. and Shiigai, H.: "On Standing Internal Gravity Waves in the Cylindrical Boundary," Proceedings of the Japan Society of Civil Engineers, No. 219, 1973, pp. 45-53, (*in Japanese*)
17) Sawamoto, M. and Kato, K.: "On Internal Standing Waves with Finite Amplitude," Proceedings of the Japan Society of Civil Engineers, No. 232, 1974, pp. 37-47, (*in Japanese*)
18) БОГОЛЮБОВ, Н.Н. и МИТРОПОЛЬСКИЙ, Ю.А.: "АСИМПТОТИЧЕСКИЕ МЕТОДЫ В ТЕОРИИ НЕЛИНЕЙНЫХ КОЛЕБАНИЙ," Kyoritsu Shuppan, Inc., Tokyo, 1961, pp. 170-272, (*translated by M. Masuko from Russian to Japanese*)
19) McLachlan, N.W.: "Theory and Application of Mathieu Functions," Dover Publications, Inc., New York, 1964
20) Ippen, A.T. (ed.): "Estuary and Coastline Hydrodynamics," McGraw-Hill, Inc., New York, 1966, pp. 61-63
21) Pierson, W.J.: "On the Propagation of Waves from a Model Fetch at Sea," Proceedings of NBS Semicentennial Symposium on Gravity Waves, 1952, pp. 175-185

List of Symbols

a_V : amplitude of the vertical tank displacement
A : horizontal cross-sectional area of a tank
A_n : coefficient determined on the rigid boundary
$A_{\mathrm{I}n}(t)$: function of t only, in the upper layer, inside a rectangular tank
$A_{\mathrm{II}n}(t)$: function of t only, in the lower layer, inside a rectangular tank
b : width at x in a tank
b' : $b'=\dfrac{db}{dx}$
b_H : amplitude of the horizontal tank displacement
B_H : mean amplitude of the horizontal tank displacement
$B_{\mathrm{I}n}(z)$: function of z only, in the upper layer, indide a rectangular tank
$B_{\mathrm{II}n}(z)$: function of z only, in the lower layer, inside a rectangular tank
$C_{\mathrm{I}n}(t)$: function of t only, in the upper layer, inside a rectangular tank

$C_{\mathrm{II}n}(t)$	: function of t only, in the lower layer, inside a rectangular tank
$D_{\mathrm{I}n}(z)$	: function of z only, in the upper layer, inside a rectangular tank
$D_{\mathrm{II}n}(z)$	: function of z only, in the lower layer, inside a rectangular tank
E	: $E=b_H\Omega^2\beta_n$
f	: frequency of wave paddle movement
f_n	: natural frequency of the fluid inside a tank
$f^*_H(s)$	: Laplace transform of $f_H(t)$
$f_H(t)$	: horizontal tank displacement
$\tilde{f}_H(t)$	: nondimensional horizontal tank displacement
$f_V(t)$	: vertical tank displacement
$\tilde{f}_V$	: nondimensional vertical tank displacement
$\boldsymbol{F}$	: external force vector
g	: gravitational acceleration
$\tilde{g}$	: nondimensional gravitational acceleration
$G_{\mathrm{I}ni}(t)$	: function of t only, in the upper layer, inside a circular tank
$G_{\mathrm{II}ni}(t)$	: function of t only, in the lower layer, inside a circular tank
h	: fluid depth
h_{I}	: thickness of the upper layer
h_{II}	: thickness of the lower layer
$H_{\mathrm{I}ni}(z)$	: function of z only, in the upper layer, inside a crcular tank
$H_{\mathrm{II}ni}(z)$	: function of z only, in the lower layer, inside a circular tank
$\boldsymbol{i}$	: unit vector in the x-direction
I_z	: $I_z=\int_A x^2 dA$
I_i	: $I_i=2k_{1i}r_0/\{(k_{1i}r_0)^2-1\}J_1(k_{1i}r_0)$
$\boldsymbol{j}$	: unit vector in the y-direction
$J_n(kr)$	: Bessel function of the first kind
$\boldsymbol{k}$	: unit vector in the z-direction
k	: $k=\pi/2h$
k_n	: n-th solution of $J'_1(k_nr_0)=0$
k_{ni}	: i-th solution of $J'_n(k_{ni}r_0)=0$
K	: $K=2\int_{-L}^{L}\frac{1}{b}\left(\int_{-L}^{x}bxdx\right)^2\left(1+\frac{b'^2}{3}\right)dx$
l	: half length of a sliced section of the tank
l_x	: length of the rectangular tank
l_y	: width of the rectangular tank
L	: half length of the tank
n	: positive integer
p_0	: preliminary weighted pressure of the fluid
p_i	: impulsive fluid pressure
p_c	: convective fluid pressure
p_{I}	: fluid pressure of the upper layer
$\tilde{p}_{\mathrm{I}}$	: nondimensional fluid pressure of the upper layer
p_{II}	: fluid pressure of the lower layer
$\tilde{p}_{\mathrm{II}}$	: nondimensional fluid pressure of the lower layer
$q(t)$	: function of t
$q^*(s)$	: Laplace transform of $q(t)$
Q	: $Q=\int_{-l}^{x}xbdx$
r	: r axis for cylindrical coordinates

r_0	: radius of the circular tank
s	: parameter in the Laplace transformation
$S(t)$	: function of t
t	: time
T_H	: mean period of the horizontal displacement
u_{I}	: velocity of a fluid particle, in the x-direction, inside the upper layer
u_{II}	: velocity of a fluid particle, in the x-direction, inside the lower layer
$u_{r\mathrm{I}}$	: velocity of a fluid particle, in the r-direction, inside the upper layer
$u_{r\mathrm{II}}$	: velocity of a fluid particle, in the r-direction, inside the lower layer
$u_{\theta\mathrm{I}}$	: velocity of a fluid particle, in the θ direction, inside the upper layer
$u_{\theta\mathrm{II}}$	: velocity of a fluid particle, in the θ direction, inside the lower layer
U	: $U=E/(\omega^2-\Omega^2)$
$\boldsymbol{v}_{\mathrm{I}}$	: velocity vector of a fluid particle in the upper layer
$\boldsymbol{v}_{\mathrm{II}}$	: velocity vector of a fluid particle in the lower layer
v_1	: velocity of a fluid particle, in the y-direction, inside the upper layer
v_2	: velocity of a fluid particle, in the y-direction, inside the lower layer
$\tilde{v}_{\mathrm{I}}$	: nondimensional v_{I}
$\tilde{v}_{\mathrm{II}}$	: nondimensional v_{II}
w_{I}	: velocity of a fluid particle, in the z-direction, inside the upper layer
w_{II}	: velocity of a fluid particle, in the z-direction, inside the lower layer
$\tilde{w}_{\mathrm{I}}$	: nondimensional w_{I}
$\tilde{w}_{\mathrm{II}}$	: nondimensional w_{II}
x	: horizontal axis of Gausian coordinate
$\tilde{x}$	: nondimensional x
X_{I}	: displacement of a fluid particle in x-direction inside the upper layer
X_{II}	: displacement of a fluid particle in x-direction inside the lower layer
y	: horizontal axis of Gausian coordnates
$\tilde{y}$	: nondimensional axis of y
Y_{I}	: displacement of a fluid particle, in the y-direction, inside the upper layer
Y_{II}	: displacement of a fluid particle, in the y-direction, inside the lower layer
z	: vertical axis of Gausian coordinates
Z_{I}	: vertical displacement of a fluid particle, inside the upper layer
Z_{II}	: vertical displacement of a fluid particle, inside the lower layer
α	: directional angle of earthquake action, measured from the x axis
α_n	: constant coefficient
β	: constant coefficient
γ	: angular frequency of the vertical tank movement
Δ	: small quantity of the angular frequency difference
ε	: nondimensional small quantity$=a\gamma^2/g$
ζ	: boundry surface displacement or water surface displacement
$\zeta_{\max}$	: propagating wave height
ζ_0	: wave height in uniform wave train
η_0	: amplitude of the boundary surface displacement, from its still position
θ	: axis of cylindrical coordinates
λ	: $\lambda=(\Omega-\gamma)t$
μ	: $\mu=(\Omega+\gamma)t$
ν	: phase difference
σ	: $\sigma=\gamma t$
τ	: $\tau=\Omega t$

Φ	: velocity potential
ψ	: phase of boundary surface displacement
Ω	: angular frequency of the horizontal tank movement
ω	: natural angular frequency